Review

Low band gap polymers for organic photovoltaics

Eva Bundgaard*, Frederik C. Krebs

The Danish Polymer Centre, Risø National Laboratory, P.O. Box 49, Frederiksborgvej 399, Roskilde, Denmark

Abstract

Low band gap polymer materials and their application in organic photovoltaics (OPV) are reviewed. We detail the synthetic approaches to low band gap polymer materials starting from the early methodologies employing quinoid homopolymer structures to the current state of the art that relies on alternating copolymers of donor and acceptor groups where strategies for band gap design are possible. Current challenges for OPV such as chemical stability and energy level alignment are discussed. We finally provide a compilation of the most studied classes of low band gap materials and the results obtained in photovoltaic applications and give a tabular overview of rarely applied materials.
© 2007 Elsevier B.V. All rights reserved.

Keywords: Low band gap polymers; Synthesis; Organic photovoltaics (OPV)

Contents

*Corresponding author.
E-mail address: eva.bundgaard@risoe.dk (E. Bundgaard).

1. Introduction

In the past decade, focus on organic photovoltaic (OPV) devices has increased and several reviews on OPVs have been published [1–8]. There are many reasons for the interest in OPVs when comparing the technology to the silicon-based photovoltaics (PV) and interestingly the two very different technologies are complementary in many ways. The OPVs offer low cost, low thermal budget, solution processing, flexible substrates and a very high speed of processing. Until recently the silicon-based PVs had advantages in both efficiency and lifetime of the device where module efficiencies in excess of 20% and operational stabilities under outside conditions of more than 25 years have been demonstrated for monocystalline silicon devices. In the 1980s and early 1990s, when the OPVs were in their infancy they showed low efficiencies and short lifetimes and were thus not a real competitor [5]. In recent years, this has changed dramatically and both the efficiency and lifetime of OPVs have improved significantly with efficiencies of around 5% and estimated operational lifetimes of 20,000 h [9–11]. It should be emphasized that high efficiency and long lifetime has not been observed for the same device, and one of the current challenges is the combination of all the desirable properties in the same material (efficiency, stability, processability and low cost). The separate demonstration of these properties for different materials, however, does show that it should be possible and from this point of view the OPVs could become a true competitor to the silicon-based PV. In addition OPVs do have advantages of better operation at low light levels (i.e. indoor applications) [12] compared with most inorganic PVs. There are several factors that influence the efficiency of OPVs, e.g. the structure of the polymer, the morphology of the film, and the choice of electron acceptor and the ratio between this and the polymer [13].

During the last decade several research groups have reported the synthesis and use of materials which absorb light with wavelengths above 600 nm in OPVs. A band gap is defined as the difference between the highest occupied molecular orbital (HOMO) and the lowest unoccupied molecular orbital (LUMO) energy levels in the polymer. Low band gap polymers are loosely defined as a polymer with a band gap below 2 eV, i.e. absorbing light with wavelengths longer than 620 nm.

In this review, an introduction to low band gap polymers is given with a detailed discussion of why we need to focus on low band gap polymers and considerations of how to design the polymer to achieve the low band gap. Further, the synthesis and PV responses of low band gap polymers from the literature are described. The polymers described have mostly been prepared by two methods: (1) electrochemical polymerization, where a potential is applied to a solution containing the monomer and an electrolyte, this results in formation of the polymer at the anode, e.g. indium tin oxide (ITO) or (2) chemical polymerization using Stille, Negishi, Kumada or Suzuki cross-coupling reactions, oxidative ferric chloride polymerizations and Yamamoto, Knoevenagel or Horner–Wadsworth–Emmons condensation polymerizations. For other reviews on low band gap polymers see [6,14–16].

2. Reasons for aiming at low band gap materials and design considerations

2.1. A view of the sun spectrum, the number of photons and short circuit current limits

The sun is a stable source of renewable energy and it is estimated to last for another 5 billion years. At the core of the sun 5 million tons of energy is released every second in the form of γ-rays, which is equivalent to 3.86×10^{26} J. The γ-rays make their way to the surface of the sun by absorption and re-emission at lower and lower temperatures until it reaches the surface mainly as the visible light we observe on earth. The energy in space just outside the atmosphere of the earth is 1366 W m^{-2} and when the light energy passes through the atmosphere part of the visible light energy is lost by absorption in specific regions of the spectrum according to the air mass that the light passes. The air mass is abbreviated AM followed by a number that describes the air mass. In space, just outside the atmosphere the spectrum is AM0. The absorption loss amounts to 28% resulting in about 1000 W m^{-2} at the surface of the earth at equator under ideal conditions with a spectrum according to the air mass (AM1). At the latitudes of northern Europe and northern America the absorption loss is higher resulting in the AM1.5 spectrum, which is shown in Fig. 1 as irradiance and it is evident that most of the intensity is concentrated below 2000 nm but extending

above 4000 nm. The AM1.5 spectrum corresponds to the solar irradiance with the sun 45° above the horizon [17]. It is, however, more relevant to consider the amount of photons available since PVs essentially convert 1 photon into one electron (there are particular cases where 1 photon can give rise to more than 1 electron but this is beyond the scope of this review). Thus, the representation of the solar spectrum in photon flux as a function of wavelength give a better picture of how many photons that are available for conversion into electrons under ideal conditions (Fig. 1). Fig. 1 shows a displacement of the maximum towards the infrared wavelengths when considering the number of photons rather than the energy. From this point of view it is of great interest to harvest photons at the longer wavelengths. It should be borne in mind that the energy of the charge carriers at longer wavelengths is lower and this limits the voltage difference that the device can produce. Thus, there is an optimum band gap which is currently subject to discussion for excitonic devices. The view taken in this account is experimental and the practical efficiencies that can be obtained for low band gap materials may not coincide with the theoretically predicted value for the optimum band gap. It is, however, important to extend

absorption beyond 600 nm. Based on these simple considerations the low band gap polymers have the possibility to improve the efficiency of OPVs due to a better overlap with the solar spectrum [17,18]. Thus, for a maximum photon harvesting in the OPV devices low band gap materials are needed [19].

In Fig. 2, the photon flux from Fig. 1 is shown along with its integral, which is shown on two different scales. One axis shows the integral from 280–4000 nm in terms of how high a percentage of the number of the available photons that can be absorbed by having a particular band gap. The second axis shows the integral in the maximum theoretical current density that can be obtained, provided that all photons are absorbed up to the band gap and converted into one electron in an external circuit that is $1\,e^-/photon$. It should thus be considered as the maximum possible current achievable. This graph is intended as a tool so that the experimenter can check own data or literature reports. If for instance a larger current density is obtained for a particular material than the curve predicts, it could be worthwhile checking the experiment once more (incident light intensity, spectrum, sun simulator, etc.). In Table 1, a few of the values have been highlighted for a quick overview.

In reality, most PVs can not efficiently make use of light energy below 350–400 nm due to absorption in the substrate and front electrodes (i.e. glass, ITO) but fortunately this part of the spectrum contains very little intensity. The range of wavelengths from 280 to 400 nm amounts to only ~1.4% of the total possible current or ~1 mA cm^{-2} in current density. From Table 1, it becomes evident that one will gain considerably in current when increasing the λ_{max} from 650 to 1000 nm, i.e. decreasing the band gap. Poly(3-hexylthiophene) has a band gap of 650 nm (1.9 eV) and thus only has the possibility to harvest up to 22.4% of the available photons giving a maximum theoretical current density of 14.3 mA cm^{-2} (Note that this may increase if the polymer is applied in a bulk heterojunction device, due to the absorption of the
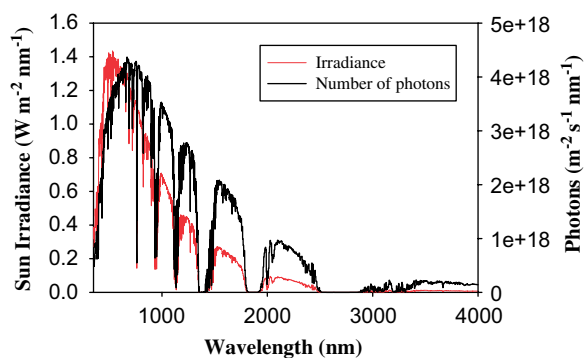

Fig. 1. Sun irradiance (red) and number of photons (black) as a function of wavelength. The sun intensity spectrum is based on data from NREL [20].
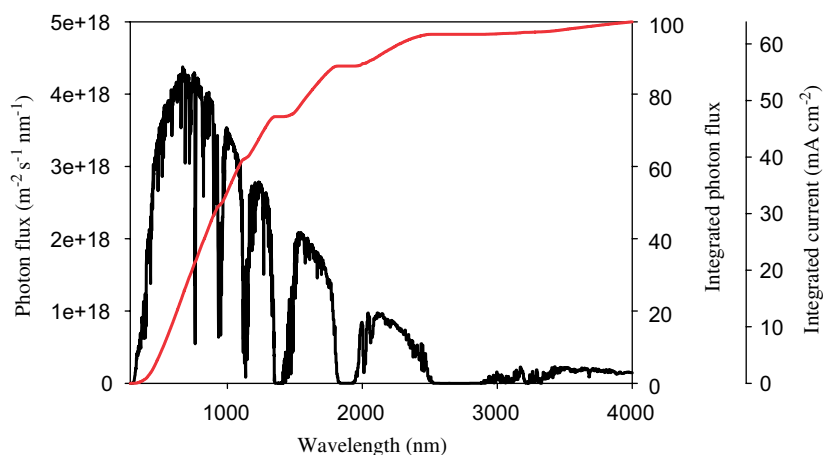

Fig. 2. Photon flux from the sun (AM1.5) as a function of wavelength. The integral of the curve is shown on the right y-axis as, respectively a percentage of the total number of photons and as obtainable current density.

acceptor, i.e. PCBM). Extending the band gap to 1000 nm will allow for absorption of 53% of the available photons giving a maximum current density of 33.9 mA cm^{-2}. In practical terms these values can not be achieved since absorption will never be complete and incident photon to current efficiencies (IPCE) will never be unity. The values, however, are good figures to have in mind as a rule of thumb when quickly evaluating literature reports or own data.

As an example we have calculated the current which can be achieved for a low band gap polymer (Fig. 3). In Fig. 3, the fraction of photons absorbed by a single passage through a film of a low band gap polymer material is shown along with the photon flux available from the sun (we do not take double passage or reflection phenomena into account). Assuming that all the absorbed photons are converted into an electron in an external circuit the maximum current can be calculated and is shown in Fig. 3 as the integral. The maximum current density that

this polymer material can produce with the absorption shown is ~12 mA cm^{-2} (Fig. 3). The current density that can be achieved, however, depends on many factors, such as morphology of the device, carrier mobility and carrier lifetime, active layer thickness, etc. The above method can give an idea of the possible current densities that can be obtained for a given material with a simple absorption spectrum of the film. However, a more useful evaluation involves performing the same calculation using an IPCE curve instead since this is a device measurement and it thus includes all the effects related to reflection, multiple passage, interference and scattering. It also includes the internal effects from morphology, carrier transport, carrier lifetime, device thickness and light absorption.

2.2. Ultimate power conversion efficiencies

In the examination of the solar spectrum above we have shown that lowering the band gap allows for absorption of more photons resulting in higher currents that can lead to higher power conversion efficiency. Two models proposed by Scharber et al. [21] and Koster et al. [22] predict that a higher efficiency of OPV devices can be achieved using a lower band gap polymer. The increase in power conversion efficiency is not granted by the current density alone, a high open circuit voltage (V_{OC}) is also needed (a high fill factor is assumed). The V_{OC} is defined in the two models as the difference between the HOMO of the donor and the LUMO of the acceptor (Fig. 4) [21,22]. For an ordinary polymer such as MEH-PVV we have $V_{OC}(1)$, now lowering the band gap, i.e. lowering the LUMO of the donor from the black line to the dotted line, does not change the V_{OC}. However, combining the low band gap with a higher LUMO of the acceptor (the grey to the dotted grey line) results in an increase of the open circuit voltage to $V_{OC}(2)$ and hence the efficiency is increased assuming that the difference between the LUMO of the donor and acceptor is large enough to insure charge separation.

Table 1
The integrated photon flux and maximum current density available for a PV that harvest light from 280 nm up to the wavelength quoted assuming that every photon is converted into one electron in the external circuit

Wavelength	Max. % harvested (280 nm →)	Current density (mA cm^{-2})
500	8.0	5.1
600	17.3	11.1
650	22.4	14.3
700	27.6	17.6
750	35.6	20.8
800	37.3	23.8
900	46.7	29.8
1000	53.0	33.9
1250	68.7	43.9
1500	75.0	47.9

The current density may increase if the polymer is applied in a bulk heterojunction device, due to the absorption of the acceptor beyond the band gap of the donor.
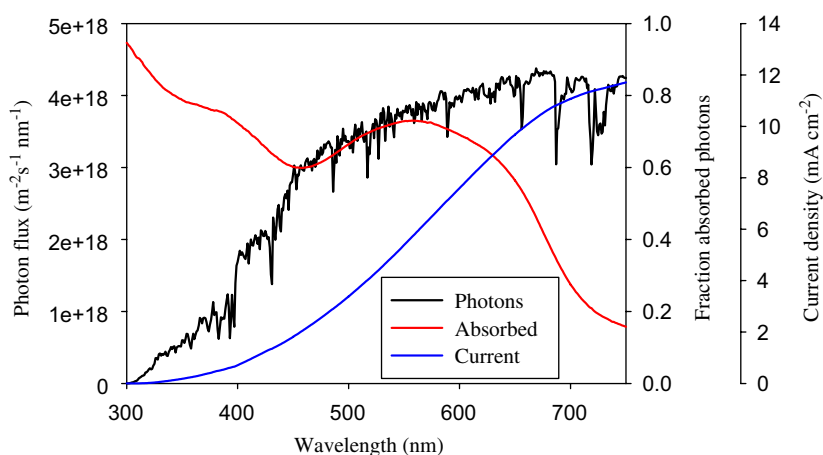

Fig. 3. Photon flux (black), photons absorbed by a copolymer of benzothiadiazole and thiophene (red) and current density (blue) as a function of wavelength. Current density is determined from the number of absorbed photons.
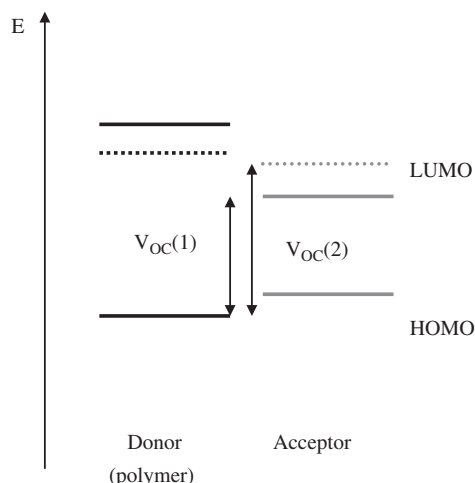
Fig. 4. Increase of V_{OC} by tuning the energy levels in a bulk heterojunction OPV device.
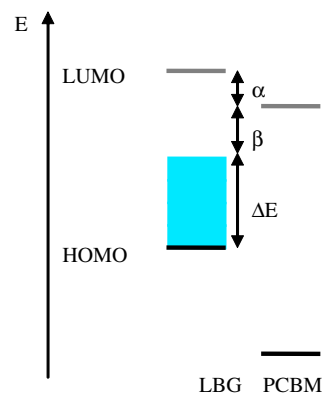

Fig. 5. Alignment of energy levels in bulk heterojunctions with a low band gap polymer (LBG) and PCBM. HOMO and LUMO are represented with thick black lines and thick gray lines, respectively. The acceptable range of energies for the HOMO level of the donor is shown as a shading.

Therefore, to increase the V_{OC} from $V_{OC}(1)$ to $V_{OC}(2)$ and thus the efficiency of the device we must prepare new low band gap polymer materials which absorb light with longer wavelengths thus absorbing more of the photons in the solar spectrum. Further, we must improve the electron transfer from the donor (polymer) to the acceptor [23]. V_{OC} can be increased by increasing the difference between the LUMO level of the acceptor and the HOMO level of the donor. Further, the LUMO levels of the acceptor and donor have to be far enough apart to guarantee energetically efficient electron transfer (see below) [21–23].

2.3. Optimum alignment of energy levels

Alignment of the energy levels in OPV is of great importance to achieve high V_{OC} and an efficient charge transport from the donor polymer to the acceptor full-erene. In Fig. 5, a schematic view of the energy levels in a bulk heterojunction is shown. The energy, α, represents the difference between the LUMO of the polymer and the LUMO of PCBM. The variable α expresses how much lower the LUMO of the acceptor PCBM is with respect to the LUMO of the donor and it has to be large enough to ensure efficient charge separation. The energy, β, represents the minimum acceptable value for V_{OC}. The choice of α and β is of course somewhat arbitrary as one would like efficient charge separation and as large a value for V_{OC} as possible and for materials with large band gaps of 2 eV or more this is not critical. There is thus a range of energies that the HOMO level of the donor material can take while fulfilling the criteria for α and β shown as ΔE in Fig. 5. When knowing the band gap of the polymer and the acceptable levels of α and β it is possible to estimate the energy range that is acceptable for the HOMO level of the donor according to: $\Delta E = E_g - \alpha - \beta$. When the band gap becomes low as in the case of low band gap polymer materials the values of the variables α and β along with the
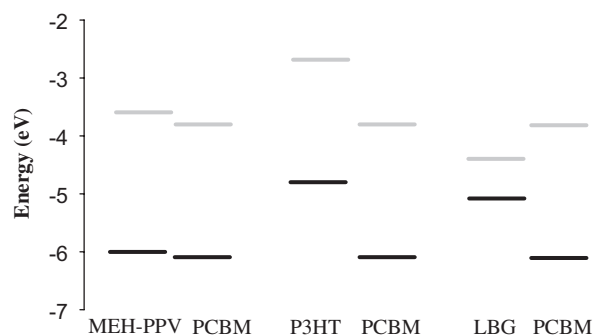

Fig. 6. Alignment of energy levels in bulk heterojunctions with PCBM using (a) MEH-PPV [24], (b) P3HT [22] and (c) low band gap polymer (LBG) [25,26].

position of the donor HOMO level becomes crucial and probably impossible in many cases if the acceptor material is chosen. Most often the range of energy levels for the acceptor is fixed as the current state of the art employ fullerene materials. This aspect underlines the need for new acceptor materials with HOMO and LUMO levels that are significantly different from the fullerenes.

In Fig. 6, examples of energy level alignment in bulk heterojunctions with PCBM and commonly used polymers, i.e. MEH-PPV (poly(2-methoxy-5-ethylhexyloxy-1,4-phe-nylenevinylene)), P3HT (poly(3-hexylthiophene)) and an example of a low band gap polymer. Fig. 6 highlights the importance of energy level alignment when using low band gap polymers compared to polymers with larger band gaps. For MEH-PPV a high V_{OC} can be achieved (see Section 2.2) and further, the alignment between the LUMO of MEH-PPV and PCBM (α in Fig. 5) can result in an efficient charge transfer. A more efficient charge transfer will result if P3HT is applied since the difference α is higher for P3HT than for MEH-PPV. However, using P3HT also decreases the maximum V_{OC}, which can be obtained.

For the low band gap polymer in Fig. 6 the LUMO energy level does not align with the LUMO of PCBM such

that an efficient charge transfer can take place. For this low band gap polymer to work efficiently in an OPV device another electron acceptor with a lower energy level of the LUMO would be required.

Thus, it is not only important to synthesize polymers with a low band gap; one also needs to consider the energy level alignment to increase the efficiency of OPV devices.

2.4. Design considerations for low band gap polymers

There are several factors that influence the band gap of a conjugated polymer material. Among these are:

(1) intra-chain charge transfer;
(2) bond-length alternation;
(3) aromaticity;
(4) substituents effects;
(5) intermolecular interactions;
(6) π-conjugation length [6,27].

Most of the low band gap polymers described in the literature are based on thiophene either as a homo polymer (polythiophene), in a copolymer or as part of a fused ring system which can be achieved by modifying the electronic properties of existing polymer units [28,29]. The low band gap copolymers reported are often based on thiophene but other electron rich aromatic units such as pyrrole are also found. Identical for these copolymers are the alternation between electron donor (electron rich) and electron acceptor (electron deficient) units [27,30]. The high energy level for the HOMO of the donor and the low energy level for the LUMO of the acceptor results in a lower band gap due to an intra-chain charge transfer from donor to acceptor [27,30]. By mathematical simulation it was shown that the electron affinity was higher around the acceptor units compared with the donor units in these types of copolymers [31–34].

Planarity along the aromatic backbone results in a low band gap, due to a high degree of delocalization of the π-electrons [35]. The alternation between single and double bonds along the polymer chain has a tendency to increase the band gap. A reduction of the difference in bond length alternation is achieved by the alternation of donor and acceptor units along the conjugated polymer chain thus lowering the band gap. In essence this concept suppresses the Peierls effect [36,37]. The alternation between donor and acceptor results in two resonance forms: D–A and $D^+ = A^-$ [35].

As described interactions between acceptor and donor enhance double bond character between the repeating units, this stabilizes the quinoid form of e.g. benzo-bis(thiadiazole) (see Fig. 29) formed within the polymer backbone, and hence a reduction in band gap is achieved [37].

If the HOMO level of the donor and the LUMO level of the acceptor are close in energy it results in a low band gap as shown in Fig. 7. Therefore, to achieve a lower band gap the strength of the donor and the acceptor must be
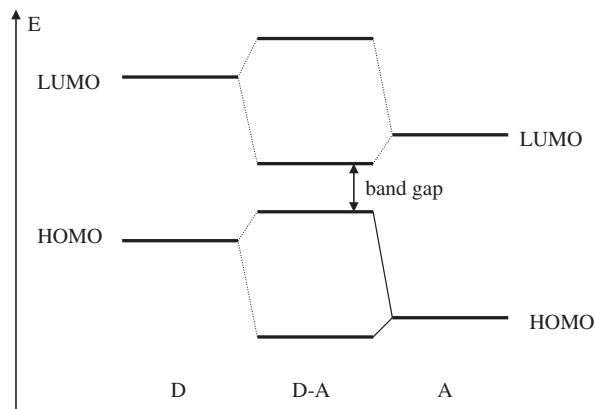

Fig. 7. Alternating donor–acceptor units lower the effective band gap by orbital mixing.

increased. This is efficiently achieved by using electron withdrawing groups (EWG) on the acceptor and electron donating groups (EDG) on the donor. EWG such as CN, NO_2, quinoxalines, pyrazines or thiadiazole lower the energy levels (and thereby LUMO) of the acceptor. EDG such as thiophene or pyrrole raise the energy levels (and thereby HOMO) of the donor [37].

It has been found that the band gap for certain polymers is lowered in the solid phase due to ordering compared to the observed disorder in solution [6,38–53]. Further, it has been found that a longer conjugation length lowers the band gap and that the band gap is increased when torsion in the polymer back bone disrupts the conjugation (see below) [6,54].

3. Types of low band gap polymers

3.1. Polythiophene

The structure of polythiophene is shown in the upper part of Fig. 8. To improve the solubility of polythiophene many different R groups have been explored ranging from alkyl, alkoxy, acid, ester and phenyl groups etc. Since the thiophene ring is a 5-membered ring that is polymerized through the 2 and 5 position substitution introduces directionality in the polymer and every time a monomer is incorporated in the growing polymer chain it can add with the head (2-position) or the tail (5-position) first.

This gives the possibility for a regular material where all the molecules add in a head to tail (HT) fashion or it can be random with occasional head to tail (HT), head to head (HH) or tail to tail (TT) coupling (Fig. 8). The lower part of Fig. 8 shows the local structure resulting from the three possible couplings.

3.1.1. Optical and electrical properties of polythiophenes

The band gap of polythiophene is 2 eV [56]. The regioregular head to tail coupled poly-3-alkylthiophene (PAT) product has a planar structure in solution and generally exhibit a lower $\pi \rightarrow \pi^*$ transition. This is an
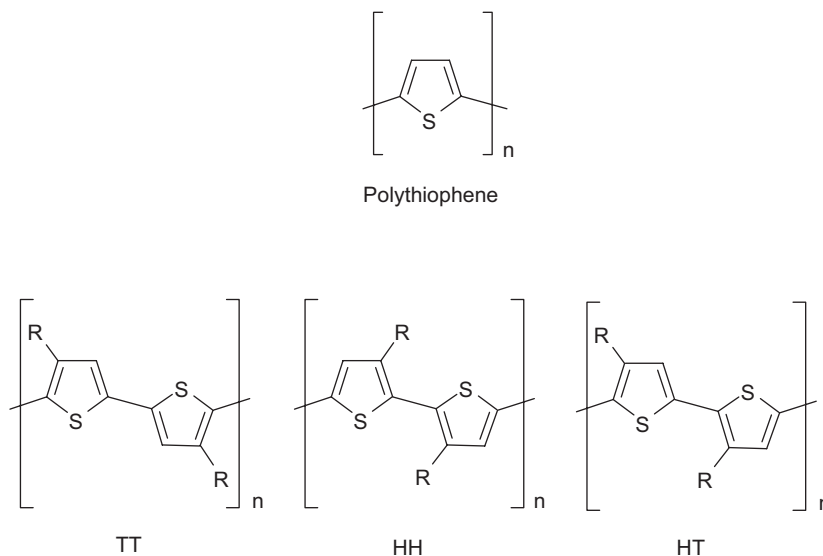
Fig. 8. Structure of polythiophene and substituted derivates of polythiophene in HH, HT and TT couplings [55].

indication of a longer conjugation length in the polymer backbone compared to regiorandom PAT (coil like structure in solution) [15]. In solution the side-chain, ordering improves with an increase in the chain length [15]. Generally, it has been established that the PAT polymer chains are straight chains with a long conjugation length both in the amorphous and crystalline phase [45,46].

Poly(3-hexylthiophene), P3HT, is one of the most studied conjugated polymers. The band gap of P3HT is 1.9 eV [22]. The λ_{max} of P3HT and for PAT in general varies with the percentage of head-to-tail coupling, i.e. the regularity of the side chains. Hence, the synthetic procedure leading to P3HT has a large influence on the properties of the final polymer product (see below) [38,57]. Further, it has been shown that the absorption of P3HT depend on the molecular weight of the polymer [39]. That is, λ_{max} increases with an increase in molecular weight and the absorption spectrum becomes broader up to 600 nm [39]. The regioregularity of P3HT is of great importance for the characteristics of the polymer such as conductivity and charge carrier mobility and transport. Several reports have investigated the regioregularity and its effect on packing of the polymer [38–53]. It has been shown that the regioregular P3HT with a head-to-tail coupling stack in lamella structure, which is separated by the side chains [41,43–45,47,48]. Hence, the length of the alkyl side chains affects the lamella structure only in the dimension of lamella thickness [47]. The solvent used for spin coating have been shown to be of great importance [41,42,46]. Films of poly(3-octylthiophene) spin coated from chloroform was found to have their side chains directed towards the substrate [46]. This was also the case for phenyl side chains [45]. It has also been shown that the drying time and drying mechanism affects the anisotropy of the polymer film [40,41].
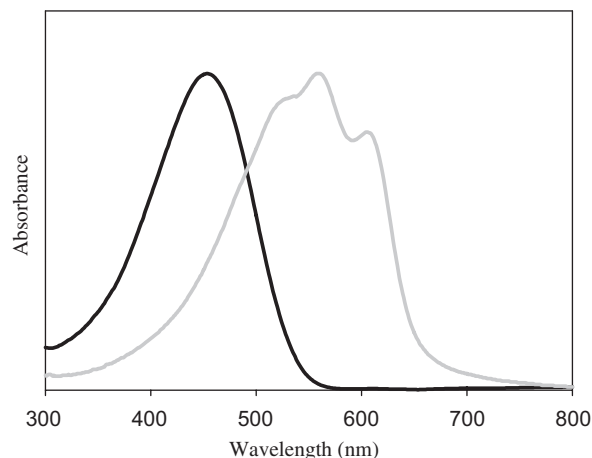

Fig. 9. Absorption spectra of regioregular P3HT in solution (black) and in a solid film obtained by spin coating from 1,2-dichlorobenzene (grey).

For P3HT or P3AT it has been found that the polymer organize in different ways in film and solution [41,42,48,58]. This is not the case for polythiophenes with phenyl side chains, which were found to organize similarly in both solution and in the solid film [42]. Furthermore, the absorption and hence the band gap of P3HT or P3AT is very different in the solid film and in solution, i.e. the λ_{max} increase when going from solution to the solid film (Fig. 9) [38]. From Fig. 9, it can also be seen that the absorption spectra for the film of P3HT is more detailed than the solution of P3HT, this is ascribed to the organization of the polymer in film.

Introduction of disorder was applied to investigate the effect of the regioregularity on the optical properties of the polythiophene [54]. P3HT was synthesized by Yamamoto polycondensation (see below) to give 91% regioregularity. The polymer was spin coated from chlorobenzene in a 1:1 mixture with PCBM, this resulted in PCBM segregation

leading to a thermally stable interpenetrating network [54]. Addition of disorder alternates the driving force for crystallization leading to thermally stable bulk heterojunctions [54]. The most stable PV performance is obtained with P3HT with tuned regioregularity to control the morphology of the bulk heterojunction [54]. This was also investigated for head-to-head coupled and tail-to-tail coupled polythiophene with different alkyl side chains [59]. It was found that the methyl side chain did not show any difference when the two couplings (i.e. HH and TT) was compared, however, when the length of the alkyl side chain increased a twist in the main chain was observed [59].
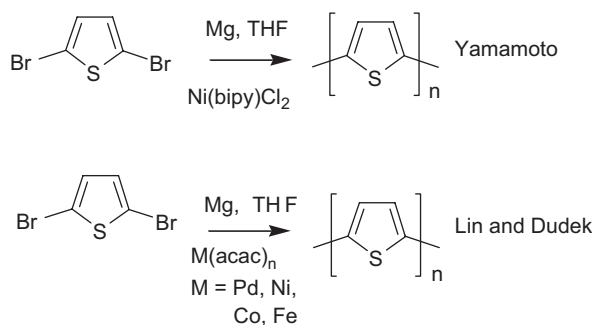

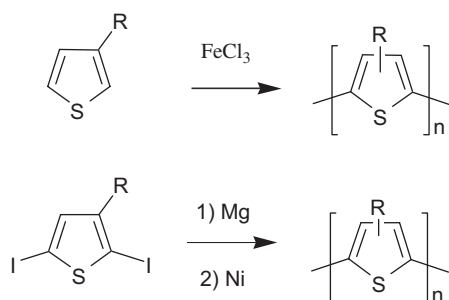Fig. 10. Synthesis of polythiophene by Yamamoto and Lin and Dudek [57,61,62].

Fig. 11. Synthesis of regiorandom PAT [55,57].

Cross-linking between thiophene units in polythiophene have been shown to increase the hole mobility in the polymer, and hence increase the efficiency of OPV devices [60]. However, a very high percentage of cross-linking resulted in a main chain distortion and poor solubility. This caused the hole mobility to decrease and thereby also resulted in a decrease in efficiency [60].

3.1.2. Synthetic strategies leading to polythiophenes

The synthesis of polythiophene has been carried out by several different strategies and the first synthesis of polythiophene was carried out by two different chemical polymerizations in 1980 by Yamamoto et al. and Lin and Dudek (Fig. 10) [61,62]. At the same time an electrochemical polymerization of thiophene was reported [14]. However, these three types of polymerizations all led to insoluble polymer products. Thus, in the late 1980s several research groups strived to prepare soluble derivatives of polythiophene [63–65]. The PAT, first described in 1986, have three conformations; HT-HT, TT-HT, HT-HH, TT-HH as described above, which can be achieved by the strategies shown in Fig. 11 [14,57].

As described above the regularity of P3HT is of great importance due to higher conductivity of the polymer and higher efficiency of OPV devices. However, the synthetic methods presented in Fig. 11 did not give a regioregular polymer product [46]. Highly regioregular P3HT was not reported until the early 1990s by McCullough [66] and Reike [67] by two related methods as shown in Fig. 12. These methods have been explored extensively [57,68–84]. The regioregularity obtained from these synthetic procedures was 99% HT and 98.5% HT, respectively [57,66,83]. The conductivity of the regioregular P3HT was 1000 S/cm compared to only 1–0.1 S/cm obtained for P3HT with a low regioregularity (58–70% HT) [57].

Regioregular P3HT have also been synthesized by Stille polymerization as shown in Fig. 13, which resulted in 96% HT in 1,2-dichloroethane or toluene [85,86]. Controlled
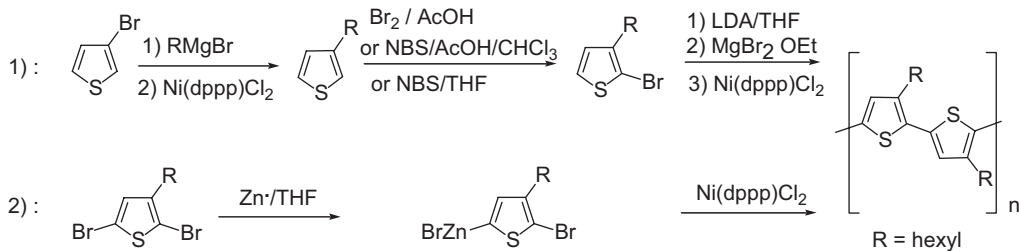

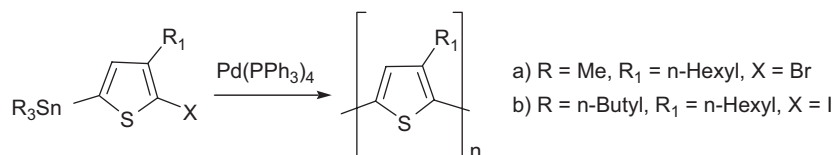Fig. 12. Different strategies to regioregular P3HT (1) McCullough and (2) Reike.

Fig. 13. Synthesis of P3HT by Stille cross-coupling polymerization [85,86].
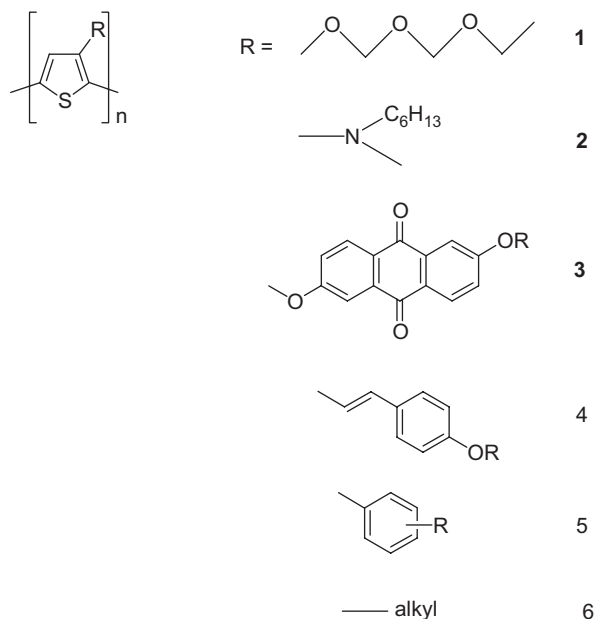
Fig. 14. Polythiophenes with different side chains: 1 [91], 2 [92], 3 [93–96], 4 [55,90,97–100], 5 [101], 6 [57], and R = alkyl-PO_3H_2 [102].

length oligomers were obtained by Suzuki cross-coupling polymerization [87].

Besides the hexyl side chain, which is the most described in the literature, several other side chains have been added to achieve polythiophenes with specific solubility properties. Some examples of these are shown in Fig. 14. Copolymers of polythiophene with different side groups, i.e. resulting in donor and acceptor units, have also been reported. Examples are: NH_2/NO_2 [88], 3 and hexyl [89] and different phenyl groups [90]. In the latter example, the absorption spectra of the copolymers in solution and in film showed a red shift of 30–50 nm for the film [90]. A further red shift was observed when the film was annealed at 130 °C for 10 min., i.e. the band gap was reduced [90]. It was shown that the solubility increases with an increase in the length of the alkyl chain [65].

3.1.3. PV devices based on polythiophenes

The first OPV device based on poly(3-methyl-thiophene) (PMET) was reported in 1984 by Glenis et al. [103]. The polymer was synthesized by electrochemical polymerization onto an ITO electrode [103]. Thereafter, gold was evaporated on top, and the result was a simple OPV device with the configuration: Al/PMET/Au [103]. The measurements were carried out with an incident light intensity of $1 \, mW \, cm^{-2}$ and a power conversion efficiency of 0.007% was achieved [103]. Since then, several groups have reported the use of polythiophenes (especially P3HT) in OPV and the highest efficiency reported to date was reported by Reyes-Reyes et al. to be 5.2% for P3HT [10]. The most commonly employed device geometry today is the bulk heterojunction. Reported applications of polythiophenes in OPV are summarized in Table 2 for P3HT

and in Table 3 for polythiophenes with side chains other than hexyl.

There are great variations in the performance of the devices shown in Table 2. However, notice the reported current densities; these have nearly reached the maximum, keeping in mind that the maximum theoretical current for P3HT with a band gap at 650 nm (1.9 eV) was found to be $14.3 \, mA \, cm^{-2}$ (AM1.5, $100 \, mW \, cm^{-2}$).

Nevertheless, there are too many variables in the experiments to allow for any reasonable comparison of the data. The purpose of Table 2 is thus to underline how many parameters that enter in device preparation and device characterization. From Table 2, it becomes evident that reported data is based on experiments that vary with respect to material source, molecular weight, solvent, annealing, electrodes, barrier layers and incident light. In addition to these identifiable differences there are many more variables that are not included in experimental descriptions either intentionally or unintentionally. It is, however, well established and generally agreed that regioregularity, molecular weight, processing solvent, annealing temperature and the substrate have a large influence on the device performance.

Schilinsky et al. showed that the PV performance was highly dependent on the molecular weight of the P3HT, and large efficiencies were only obtained for samples with a high molecular weight ($M_n > 10,000$) [39]. The molecular weight has been shown to affect absorption properties, as detailed above, showing an increase in conjugation with an increase in M_n [124]. However, recent results suggest that in bulk heterojunction devices with PCBM a certain interplay between the highly regioregular, high molecular weight material and a low molecular weight material of low regioregularity may be important as a contact material or "glue" in the interface between the crystalline P3HT domains and the PCBM nanocrystals [122]. Besides the molecular weight the regioregularity influences the responses of the OPV [103]. Thus, it has been the aim for several research groups to use polythiophene with high degree of regioregularity in OPV devices, as described above (Table 2).

3.1.4. Interface layers and stability of polythiophene based OPVs

Several research groups have reported devices where layers between the electrodes and the active layer have been employed to improve the charge transport (Table 2). Examples are layers of lithium fluoride (LiF) between the active layer and Al [10,105,107,112,116,118] and transition metal oxides (i.e. MoO_3) between the active layer and ITO [108]. These are believed to increase the efficiency of the OPV device. The focus of most research groups is currently on the PCE that can be obtained for the devices. Another problem is the stability of the devices during operation. Very few research groups have focused on the lifetime of the OPV based on polythiophenes, and in the papers summarized in Tables 2 and 3 lifetime data are only reported in two instances [9,116]. Yang et al. documented

Table 2
Photovoltaic responses obtained for poly(3-hexyl-thiophene), P3HT

M_w (M_w/M_n)	P3HT/PCBM	Solvent	Area (cm²)	Annealing temperature (°C)	I_{SC} (mA cm⁻²)	V_{OC} (V)	FF (%)	η (%)	IPCE/λ (%, nm)	Notes	Refs.
RM:	—	DCB	0.05–0.08	75 (4 min)[a]	8.5	0.55	60	3.5	70/500	800 W m⁻²	[105]
RM: 30000	1:1	DCB	0.11	110 (10 min)	10.6	0.60	67.4	4.4	63/500	Ca/Al	[106]
RM: 87000	1:1	—	0.148	155 (2–3 min)	10.1	0.86	61	5.2	—	80 mW cm⁻²	[10]
RM:	1:0.8	CB	0.148	150 (30 min)	9.5	0.63	68	5.0	60/500[b]		[11]
RM:	1:2	THN	0.025–0.04	120 (10 min) 100 (5 min)	11.8	0.54	56	3.6	—		[107]
RM: 30000	1:1	DCB	0.105	110 (10 min)	8.94	0.6	61.9	3.33	63/500	ITO/MoO₃ (5 mm), Ca/Al	[108]
RM:	1:1	CHCl₃		130 (20 s)	6.35	0.60	63	2.39	62/500	Xe-lamp	[109]
RM:	1:2	CB	0.02	75 (4 min)	15.2	0.54	37[c]	—	15/340 65/540		[110]
AD: 36000 (1.9)	1:2 PCBG	DCB	—	140 (4 min)	5.2	0.53	62	>2	—		[111]
AD:	1:2	Toluene	0.09	96 (1 min)	8.16	0.58	45.5	2.15	8/475	PET substrate	[112]
MK: 44000–28000	1:1	CB	0.045	50 (30 min), 140 (4 min)[d]	0.85	0.6	—	1.14	35/500		[113]
—	35:1 (C₆₀)	CN/BFEE (1:2)	0.09	No annealing	0.3	0.81	38	0.3	—	Electrochemical polymerisation,[e] Ca/Ag	[114]
—	1:3	—	0.04	—	8.7	0.58	55	2.8	76/550	50 mW cm⁻², Ca/Al	[115]
100000 (2.14)	1:1	DCB	1.0	120 (60 min)	7.2[f]	0.615	61	2.7	56/500		[116]
19000	1:1	CB	4	80 (30 min)	9.9	0.60	41	2.41	60/550	Mg/Al	[117]
52100 (2.19)	1:1	CB	0.06–0.08	120 (4 min)[g]	5.64	0.58	62	2.09	30/500	97 mW cm⁻²	[118]
19000 (1.35)	1:1	Xylene	0.04	—	10	0.6	55	3.2	55/550	Ca/Ag	[39]

The measurements were carried out at 100 mW cm⁻² and AM1.5 unless otherwise noted. Polymer purchased from: RM = Reike Metals and Aldrich (M_w = 15000 in THF [67]), AD = American Dyes source (M_w = 20000–50000 [104]), MK = Merck. Solvent: DCB = 1,2-dichlorobenzene, CB = chlorobenzene, THN = tetrahydronaphthalene, CN = 1-chloronaphthalene, BFEE = boron trifluoride diethyl ether complex. The structure of the devices was: ITO/PEDOT:PSS/pol:PCBM/LiF/Al.
[a]The device was treated with 2.5 V before the IV measurements to burn shunts in the device.
[b]With a layer of TiO₂ between the Al electrode and the active layer the IPCE was increased to 90% at 500 nm [119].
[c]Layer investigations for this device showed an increase in I_{SC} but a decrease in FF with an increase in thickness.
[d]Annealing: at 50 °C for 30 min before deposition of Al electrode and at 140 °C for 4 min after deposition in air.
[e]The polymer was synthesised by electrochemical polymerisation with 8 mmol thiophene and 2.3 mmol C₆₀ in CN/BFEE (1:2).
[f]Calculated from IPCE.
[g]The device was annealed before deposition of the LiF/Al electrode.

Table 3
Photovoltaic responses obtained for other polythiophenes

Polymer/ PCBM	Solvent	Area (cm^2)	Annealing temperature (°C)	I_{SC} (mA cm^{-2})	V_{OC} (V)	FF (%)	η (%)	IPCE/λ (%, nm)	Notes	Refs.
C$_{60}$	Toluene	10	200 (15 h)[a]	1.05	0.505	29	0.167	—	Lifetime > 20000 hours	[9]
C$_{60}$	Toluene	—	—	0.09	0.53	33	0.15	—	P3OT, 10 mW cm^{-2}	[120]
—	Xylene	—	No anneal	11	0.6	—	3.59	—	P3HT fibers	[121,122]
1:1 (C$_{60}$)	Xylene	12	—	1.06	0.6	30	1.5	20/488	Flexible, P3OT 10 mW cm^{-2}	[1,123]
1:2	DCB	—	—	1.52	0.63	37	0.54	—	Ca/Al 70 mWcm^{-2}	[97]

The measurements were carried out at 1000 Wm^{-2} and AM1.5 unless otherwise noted. The structure of the devices was: ITO/PEDOT:PSS/pol:PCBM/Al, no PEDOT: PSS.
[a]Thermocleavage of ester side chains to acid side chains before deposition of C$_{60}$ and Al.

a very good morphological stability for a P3HT/PCBM bulk heterojunction device when tested under accelerated conditions by illumination with incident light intensity of 1000 W m^{-2} (AM1.5) at 70 °C in a glovebox [116]. A second example of a polythiophene device with a very long lifetime was obtained by making devices via solution processing of a polythiophene with a tertiary alkyl ester side chain. The side chain could be removed by a thermal treatment giving a more stable device. A tremendous increase in the lifetime of a 3 cm^2 device (ITO/P3CT/C$_{60}$/Al) was reported [9]. The efficiency for this type of device was upto 0.17% and the lifetime was estimated to be 20,000 h through accelerated tests [9].

3.1.5. Morphology of the active layer in polythiophene based OPVs

There are several factors that influence the morphology of the active layer in OPV devices [13]. It has been shown that a good morphology, i.e. a smooth film, increases the efficiency of the device. For P3HT the dependence of the PV response on molecular weight [53], annealing temperature (Table 2) and solvent [125] have been carried out.

In Table 2, it can be seen that the various research groups employ different solvents for spin coating the active layer, and it has been shown that the evaporation time of the solvent has a large influence on the morphology of the active layer [108].

Morphology studies carried out with two different acceptors: PCBM and PCBG (see Fig. 40), showed that PCBG (phenyl-C$_{61}$-butyric acid glucidol ester) stabilizes the morphology of blends with P3HT upon annealing preventing phase separation [111,126]. In P3HT/PCBM blends used in bulk heterojunctions it has been shown that the hole and electron mobility depends on the content of PCBM [50,127]. An increase in the PCBM content increases the electron mobility while the hole mobility decreases only slightly [50,127].

Studies of the influence of the film thickness on the PV responses shows that to achieve a high IPCE > 90% the thickness of the active layer, with P3HT and PCBM, has to be 240 nm [23], and further that the replacement of MEH-PPV with P3HT in OPV results in a better hole transport [23,105]. It was found that an IPCE of 70% could be achieved at λ_{max} [23,105]. The effect on crystallinity of annealing and the P3HT/PCBM ratio showed that the mean drift length of photogenerated charge carriers exceeds the active layer thickness under PV operation. Hence, when the thickness of the active layer is increased the I_{SC} increases due to improved light absorption [128].

Investigations on OPV (ITO/PEDOT:PSS/polymer:PCBM/ LiF/Al) shows that V_{OC} varies with the variations in oxidation potential of the donor polymer, i.e. polythiophene with different phenyl groups [98]. When P3HT (95.4% HT)/PCBM with a 1:1 ratio was spin coated from chlorobenzene it was found that the highest efficiency (4.4%) was achieved for the highest regioregularity [129].

The photoluminescence of polythiophenes [130] and the photoluminescence (PL) quenching of mixtures between P3HT and C$_{60}$ [96] has been studied extensively as the PL quenching mechanisms has been linked to the processes of charge carrier of other substituted polythiophenes [130].

3.1.6. Hybrid solar cells and tandem cells based on polythiophenes

We have limited the results presented in Tables 2 and 3 to organic bilayer and bulk heterojunction devices. Devices based on mixtures of polythiophenes with inorganic n-type semiconductors have also been reported. These types of devices are generally termed hybrid solar cells and typical examples are based on mixtures of P3HT with CdSe, TiO$_2$, GaAs, ZnO. We have chosen not to discuss these devices here but a summery can be found in the literature [23,131,132]. Further, few reports on OPVs based on mixtures between carbon nanotubes and polythiophenes [133] or with P3HT [134], polythiophenes attached to fullerenes [135–137], the use of plasticizers such as propylene carbonate [138], other fullerenes [139] and tandem PV devices with MDMO-PPV [140] or ZnPc [141] can be found in the literature.

3.2. Poly(3,4-ethylenedioxythiophene) PEDOT

PEDOT is normally used in its oxidized form with polystyrenesulfonic acid as the anion (PEDOT:PSS) as shown in Fig. 15 [8,142]. PEDOT:PSS is used as a hole conducting and transporting layer in electroactive devices and OPVs to improve the performance [8,143–146] and has found widespread application. In addition the PEDOT:PSS complex also serves as a smoothing layer between the ITO electrode and the active layer in OPV devices and thus PEDOT:PSS have been applied in almost every OPV described in the literature (Table 1–8). Examples of conjugated polymers where 3,4-ethylenedioxythiophene (EDOT) has been incorporated in the backbone of a conjugated copolymer with thienopyrazine [147–148], isothionaphthene (ITN) and benzothiadiazole [149] and as cyanovinylene coupled polymers [150] have been described in the literature.

It has been shown that replacing ITO with PEDOT:PSS is sufficient to give low cost, flexible OPVs [143,151,152]. This is seen for doped states of PEDOT:PSS e.g. with sorbitol which results in higher conductivity [143,151]. Further, PEDOT:PSS have been shown to be highly anisotropic and uni-axial with the optical axis parallel to the surface [153]. PEDOT:PSS can be processed into uniform transparent films when spin coated from its dark blue aqueous dispersion/solution and it can be patterned to give different device structures [143,154].
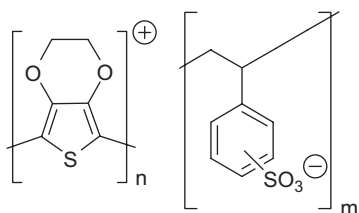

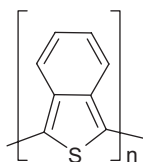Fig. 15. Structure of poly(ethylene-dioxy-thiophene): polystyrenesulfonate complex, PEDOT:PSS.

Fig. 16. Structure of polyisothianaphthene, PITN.

3.3. Polyisothianaphthene (PITN)

Isothianaphthene (ITN) is a thiophene ring with a fused benzene ring in the 3 and 4 positions as shown in Fig. 16 [28,155,156].

3.3.1. Electronic properties of PITN

The different resonance structures of PITN are given in Fig. 17. The last resonance structure is a quinoid form which is characteristic for these types of polymers [6,155,156].

The quinoid form of PITN has different energy levels for the HOMO and LUMO compared to the aromatic form of the polymer [6]. This causes the decrease in band gap which is observed [6,155]. The band gap of PITN was determined by electronic spectroscopy to be 1 eV [157]. Due to the many resonance structures of PITN and especially due to the increase in the quinoid structure in the backbone of PITN and the larger polarization causes the band gap of the polymer to decrease [157]. This is also seen for other conjugated polymers based on aromatic rings [157]. A ^{13}C NMR model simulated that PITN show a strong quinoid character [158]. Substitutions with EWG or EDG did not show any significant effect on the band gap [28].

Addition of further benzene rings as shown in Fig. 18 resulted in a larger band gap due to the increase in electron delocalization over the aromatic system and a suppression of the quinoid structure [159]. Derivatives of PITN where alkyl, alkoxy and halogen groups have been added to the backbone have been found to increase the solubility and hence the polymer is more proccessable [160].

PITN in its doped form is a highly transparent, highly conducting polymer with a conductivity of up to $50 \, \Omega^{-1} \, cm^{-1}$ for a highly doped thin film [157].

3.3.2. Synthesis of PITN and its derivatives

The synthesis of PITN was first described in 1984 by Wudl et al. [155] and two different methods have been reported:

(1) Electrochemical polymerization using lithiumbromide in acetonitrile by applying a potential (1.5 V) [155].
(2) Chemical cationic oxidative polymerization with sulfuric acid, aluminum chloride or TCNQ [155].

These pathways are quite possibly not suited for an industrial scale since the monomers and starting materials
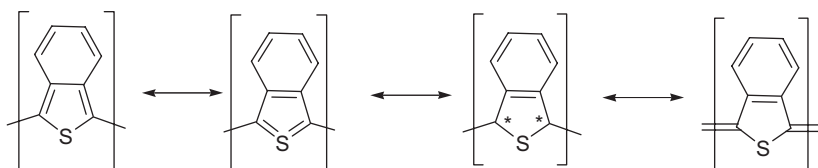

Fig. 17. Resonance structures in PITN. The stars in the third resonance structure corresponds to radicals.

are difficult to obtain, unstable and derivatives are only obtained by circuitous synthetic strategies [161]. Therefore, the synthesis of PITN from phthalic anhydride or phathalide using P_4S_{10} was described [161,162]. The reaction was carried out in xylene at 140–145 °C as shown in Fig. 19 and further the synthesis to give easy access to soluble derivatives of PITN with different alkoxy groups was described [163]. The differently substituted materials showed no significant differences in the band gap which remain ~1 eV [162].

In 2003, Polec et al. described the synthesis of soluble derivatives of PITN [163] by a non-oxidative thermal polymerization. The soluble monomer was obtained from 4,5-dichlorphtalic acid in eight synthetic steps or from 5,6-dioctyloxydithiophthalide in seven synthetic steps with pTsOH · xH$_2$O in xylene at 155–160 °C as shown in Fig. 20. The polymer had a band gap of 1.2 eV [163].
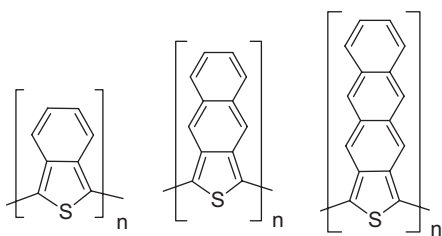
Chen et al. reported the dehydrogenation to achieve PITN as shown in Fig. 21 [164,165], where the first step was carried out by a cationic polymerization of ITN followed by the dehydrogenation [155,164,165].

In 2001, Meng and Wudl [160] described the synthesis of a soluble derivative of PITN with an electron withdrawing alkyl substituted imide group, poly (2-ethyl-hexyl-imide-isothianaphthene), PEHI-ITN (Fig. 22). The imide was introduced to change the position of the HOMO and LUMO levels and to stabilize the n-doping of PITN [160]. The polymerization was carried out oxidatively using ferric chloride from the monomer which was synthesized in 7 steps from 3,4-dimethylbutadiene and maleic anhydride [160].

3.3.3. Application of PITN in OPVs

The use of PITN and its derivatives in OPV devices have only been reported in a few instances. This can be ascribed mainly to the poor properties of PITN, i.e. low solubility and hence the polymer is not processable and further the polymer is infusible [163]. After the synthesis of a soluble derivative of PITN [163] was reported PV devices were prepared by Goris et al. [166] in 2003 and by Henckens et al. [167] in 2004. The results of these devices are summarized in Table 4.

The V_{OC} and I_{SC} given in Table 4 are very low and the highest efficiency is 0.008% [167]. This is mainly ascribed to properties of the polymer described above which results in rough films. This morphology results in shunts, poor diode behavior and rectification [166]. The addition of PCBM results in a higher current, due to better electron transport, however, the results are still very poor [166]. No further details on the application of PITN in OPV devices have been published.

Fig. 18. Structure of PITN, poly(naphthothiophene) and poly(anthracenothiophene) [159].

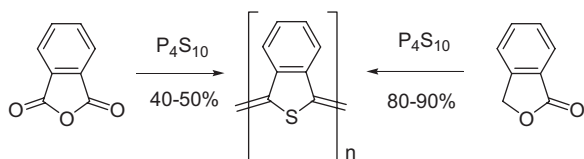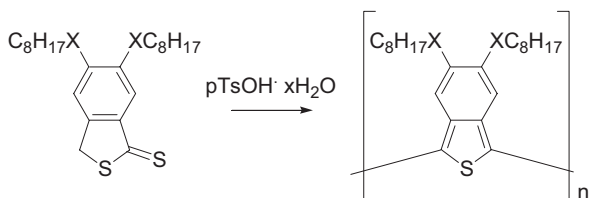Fig. 19. Synthesis of PITN from phthalic anhydride or phathalide.

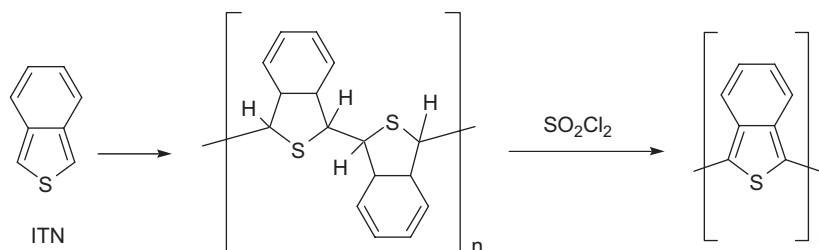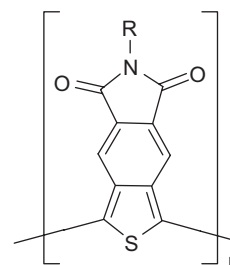Fig. 20. Synthesis of a soluble derivative of PITN [163]. X = S, O.

Fig. 22. Structure of poly (2-ethyl-hexyl-imide-isothianaphthene), PEHI-ITN.

Fig. 21. Synthesis of PITN using SO_2Cl_2 [164,165].

Table 4
Photovoltaic responses obtained for PITN and copolymers based on ITN

Polymer	Polymer/PCBM	Area (cm^2)	Annealing temperature (°C)	I_{SC} (mA cm^{-2})	V_{OC} (V)	FF (%)	η (%)	IPCE @ λ (%, nm)	Notes	Refs.
PITN	Pristine	—	—	0.01	0.35	—	—	—	Octyl, LiF/Al	[166]
PITN	1:1	—	—	0.04	0.20	—	—	0.3/700	Octyl, LiF/Al	[166]
PITN	—	—	—	0.05	0.55	30	0.008	—		[167]
P(T-ITN-T)	1:3	—	—	1.6	0.26	37	0.15	>40/450	PMMA blend	[168]
P(T-ITN-T)	1:3	—	50 during measurement	1.13	0.88	25	0.31	20/480	PMMA blend	[169]

The measurements were carried out at 80 mW cm^{-2} and AM1.5 unless otherwise noted. The structure of the devices was: ITO/PEDOT:PSS/pol:PCBM/Al.
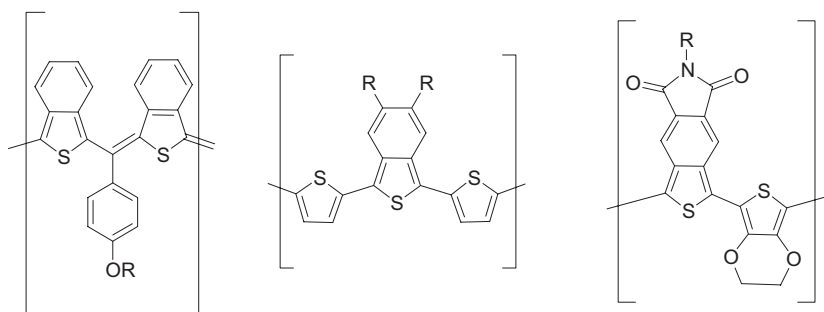

Fig. 23. Copolymers based on ITN with aromatic [19,170,171], thiophene where R = alkyl or chlorine [168,169,172,173] and EDOT [174–176].
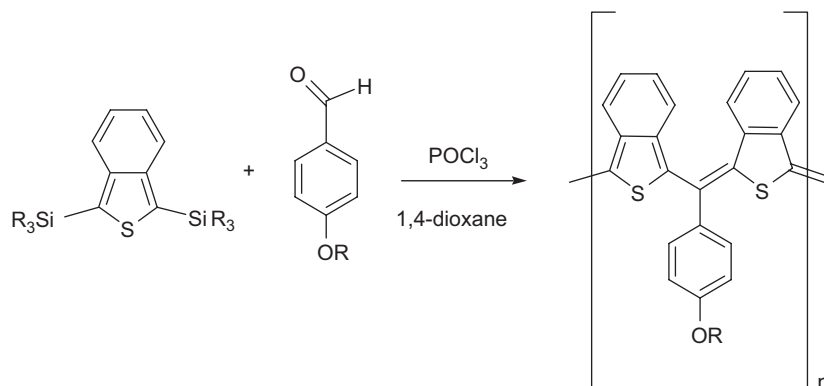

Fig. 24. Synthesis of copolymers based on ITN and aromatic units. R = alkyl.

3.4. Copolymers based on ITN

There are a few examples of copolymers based on ITN that have been published as shown in Fig. 23 [19,168–172]. In these polymers ITN is the electron acceptor and the benzylic unit [19,170,171] or the thiophene unit [168,169,172] is the electron donor.

The polymer on the left-hand side of Fig. 23 was synthesized by a coupling between a bis(trialkylsilyl) derivative of ITN and a benzaldehyde derivative by reaction with POCl$_3$ as shown in Fig. 24 [170,171]. The bis(trialkylsilyl) derivative of ITN was synthesized in 3 steps from phthalic anhydride [170,171]. The solubility of the copolymer was ensured by the alkoxy group on the

benzene ring. The band gap of the polymer was found to be 1.2–1.3 eV [170,171]. However, the polymer product exhibited a very low conjugation length due to a non-planar configuration. Hence, the charge carrier mobility was expected to be low [19].

The copolymer shown in the middle of Fig. 23, P(T-ITN-T), was first synthesized by electrochemical polymerization in 1992 [177]. Years later, in 2001, the copolymer was synthesized by oxidative ferric chloride polymerization from the monomer, which was obtained in 4 steps from 4,5-dichlorophthalic acid [169,172]. The substituents on the benzene ring of ITN were either alkyl chains [168] or chlorine [169,172]. The band gap of the resulting polymers was found to be 1.5 eV [168] and 1.76 eV [169,172],

respectively. The polymer was applied in OPV devices and the results are summarized in Table 4. From Table 4 it is clear that the efficiency has increased tremendously when comparing the copolymers based on ITN with PITN. This is due to the addition of the thiophene units, i.e. the electron donating groups. Further, it is shown that the chlorine atoms on the benzene rings result in a higher efficiency. This is ascribed to the electron affinity of chlorine and hence, the ITN unit becomes a stronger electron acceptor when comparing with the copolymer having alkyl chains on the benzene ring.

The copolymer shown on the right in Fig. 23 was synthesized by a Stille cross-coupling between a di-bromoderivative of ITN-imide and a bis(trialkylstannyl) derivative of EDOT [175]. The band gap was found to be 1.0 eV with a λ_{max} at 807 nm and a tail that extended to 1240 nm [174–176]. The low band gap of the copolymer was achieved, due to the low lying LUMO levels in ITN-imide and the high lying HOMO level of EDOT. The polymer was found to be highly stable towards n- and p-doping [174], and bulk heterojunctions of the copolymer and PCBM showed an IPCE of 3.5% at 700 nm [176]. While this is a low value compared to P3HT/PCBM bulk heterojunctions it shows that it is possible to achieve significant IPCE values with low band gap materials.

3.5. Copolymer of benzothiadiazole, pyrole and thiophene, PTPTB

Another example of an alternating copolymer based on electron donor and acceptor units are the polymer, PTPTB, shown in Fig. 25. It is based on benzothiadiazole as the electron acceptor and the block of thiophene and pyrrole as the electron donor. It has a maximum absorption around 650 nm and a strong red shift (90–100 nm) is observed when
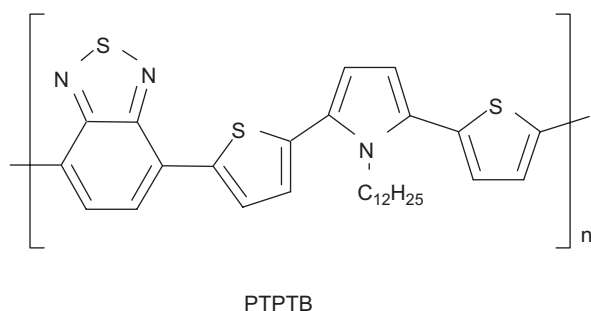
comparing the absorption spectra of solutions and films of the polymer [17]. The band gap of the polymer varies with the length of the oligomers and for the longest oligomer synthesized the band gap was 1.6 eV [17,18]. Cyclic voltammetry in dichloromethane showed $E_{ox} = 0.53$ V, $E_{red} = -1.24$ V [18,178]. The position of the HOMO and LUMO was determined by electrochemical voltage spectroscopy (EVS) to be -5.3 and -3.5 eV, respectively, and the energy levels in OPVs shows good overlap between the polymer and the electrodes [178,179]. Copolymers of pyrrole and benzothiadiazole were found to have a band gap of 2.03 eV [180].

The effect of the side chain on the nitrogen atom in the pyrrole ring caused an increase in the band gap from 1.2 to 2.0 eV [181–183]. Addition of octyl side chains on thiophene, attached to achieve solubility, resulted in a larger torsion strain due to steric hindrance and thus caused the band gap to increase [30]. PTPTB was also prepared with thermocleavable side chains on the thiophene units, which showed a significant decrease in band gap upon thermocleavage from 2.14 to 1.69 eV [180].

The copolymer was synthesized by Stille cross-coupling polymerization between a di-bromo derivative of benzothiadiazole and a di-stannyl derivative of bis-thienyl-pyrrole as shown in Fig. 26 [17,184]. The Stille cross-coupling polymerization resulted in a mixture of shorter oligomers with imperfections in the polymer chain due to chain termination, destannylation, debromination, homocoupling and methylshift [17]. The polymers were purified by Soxhlet extraction. However, the ratio of the two monomers in the reaction mixture resulted in two different fractions, and it was found that an excess of the distannyl derivative of di-thiophene-pyrrole led to longer oligomers [17].

Since it was shown that the Stille coupling resulted in short chain oligomers with low molecular weight, PTPTB was synthesized by a Suzuki cross-coupling polymerization between aryl bis-boronic acid derivatives and dihaloarenes to give soluble high molecular weight polymers (Fig. 27) [30].

Several research groups have reported on the use of PTPTB in OPV devices and the results are summarized in Table 5. The low FF and low efficiency seen in Table 5 was not ascribed to a large serial resistance but was mainly ascribed to the low molecular weight of the oligomers. This resulted in thin low-quality films and hence, a poor morphology that was also observed in AFM images [185,186]. Further, the LUMO of the polymer and the LUMO of PCBM are very close (3.7 eV for the polymer

PTPTB

Fig. 25. Structure of the copolymers based on thiophene, pyrrole and benzothiadiazole.
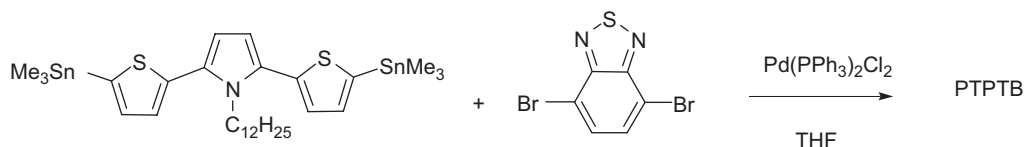

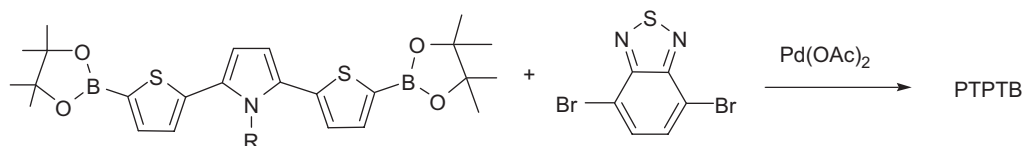Fig. 26. Synthesis of PTPTB by Stille cross-coupling polymerization.

Fig. 27. Synthesis of PTPTB by Suzuki cross-coupling polymerization, R = dodecyl.

Table 5
Photovoltaic responses obtained for copolymers based on benzothiadiazole, pyrrole and thiophene, PTPTB

Polymer/ PCBM	Area (cm^2)	Annealing temperature (°C)	I_{SC} (mA cm^{-2})	V_{OC} (V)	FF (%)	η (%)	IPCE @ λ (%, nm)	Notes	Refs.
1:1	0.1	—	—	0.70	35	0.34	—	55 mW cm^{-2}	[18]
1:1	0.1	—	0.8	0.67	35	0.34	7/600	55 mW cm^{-2}	[17]
1:1	0.1	55 during measurement	3.1	0.72	37	1.00	20/550		[187,188]
1:1	0.05	—	2.25	0.53	32	0.48	9/550	Nile red (10%)	[186]
1:1	0.05	—	1.0	0.51	30	0.20	9/500	MDMO-PPV (1:1)	[186]

The measurements were carried out at 80 mW cm^{-2} and AM1.5 unless otherwise noted. The structure of the devices was: ITO/PEDOT:PSS/pol:PCBM/ LiF/Al.

and 4.0 eV for PCBM), which caused a decrease in the selectivity of the metal electrode contacts, hence, the diode quality was low due to recombination [186,187]. It is interesting to note that the series resistance was measured to be $< 10 \Omega$ cm^{-2} while this does not explain the low FF [186,187].

The use of Nile red lowers the PV responses as seen in Table 5. This was ascribed to the additional transport step for the electron [186]. The blend with MDMO-PPV increases the rectification but reduces the PV responses under illumination. Investigations of absorption and IPCE showed that PTPTB does not contribute to the photocurrent [186].

3.6. Copolymers based on thiophene, benzothiadiazole or benzo-bis(thiadiazole)

The copolymer based on thiophene, benzothiadiazole or benzo-bis(thiadiazole) is another example of an electron donor–acceptor alternating polymer. Again the thiophene is the electron donor unit and here benzothiadiazole or benzo-bis(thiadiazole) is the electron acceptor unit. The structures of the different copolymers are shown in Fig. 28, where R represents either alkyl or alkoxy chains to achieve a soluble polymer [25,189–191].

For the copolymer based on thiophene and benzothiadiazole results have shown that the number of thiophenes between the benzothiadiazole units affects the band gap of the polymer [25]. Thus, it was possible to tune the band gap of the copolymer with the number of thiophene units between the benzothiadiazole units from 2.1 eV for one thiophene to 1.65 eV for four thiophenes [25]. This is

ascribed to an optimization of the donor properties of the oligothiophene donor segment with respect to the acceptor unit and for this reason there is an optimal length of the oligothiophene segment for a given acceptor unit such as benzothiadiazole. Increasing the number of thiophenes beyond the optimum will gradually approach the band gap of polythiophene [25]. The low band gap of these types of copolymers based on either benzothiadiazole or benzo-bis(thiadiazole) are ascribed to the strong quinoid form of the polymer as shown in Fig. 29 which contributes to the low band gap due to the more stable 1,2,5-thiazole which is formed [29]. Further, the polymer shows a planar geometry, which result in non-steric repulsion between the two heterocycles. The polymer has a high electron affinity due to the sulfur atoms in the thiadiazole rings and the short intermolecular contacts between S and N results in strong inter chain interactions [29]. It was found that the benzo-bis(thiadiazole) unit showed the highest electron-accepting ability among thienopyrazine, pyrazino-quinoxaline and benzothiadiazole and that this also resulted in the lowest band gap [27].

The use of sidechains is essential to make the polymer soluble enough for application in OPVs by for instance spin coating [25,189]. However, the side chains often introduce steric hindrance affecting the coplanarity of the polymer and hence, the band gap of the polymer increases [189]. Further, the side chains can affect the regularity of the structure when applied in different positions in the polymer [189]. This can be seen for the copolymers with R = H, where the band gap was found to be 1.1 eV for the copolymer based on di-thiophene and benzothiadiazole
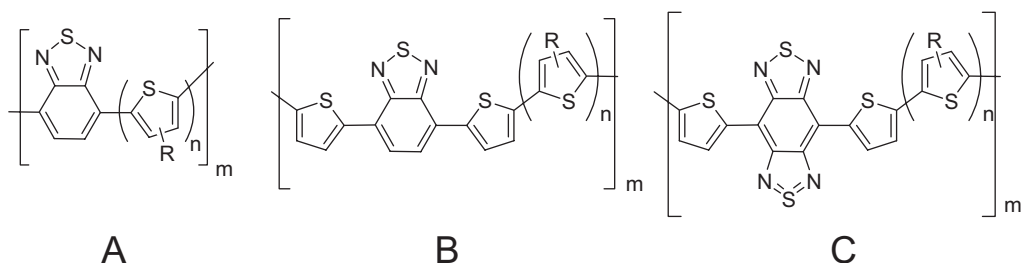
Fig. 28. Structure of copolymers of thiophene and benzothiadiazole or benzobisthiadiazole. R = alkoxy for A: $n = 2$ [191], R = hexyl for A: $n = 2$, B: $n = 2$ and C: $n = 2$, R = 2-ethylhexyl for A: $n = 1$, B: $n = 1, 2$ and C: $n = 1$, R = dodecyl for B: $n = 2$, R = 3,7,11-trimethyldodecyl for A: $n = 1, 2$, B: $n = 1, 2$ and C: $n = 1,2$ [25,190].
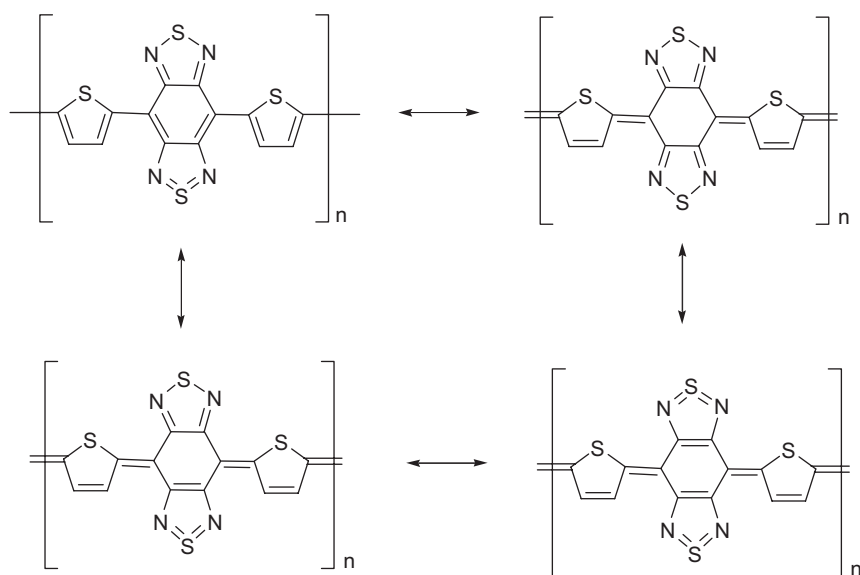

Fig. 29. Resonance structures in benzo-bis-thiadiazole.

[29] and below 0.5 eV for the copolymer based on dithiophene and benzo-bis(thiadiazole) [29].

Mullenkom et al. have predicted that to achieve absorption maxima of less then 1 eV for a donor-acceptor copolymer the codimer D–A must have absorption maxima at 550 nm (2.2 eV) [181]. This is not seen for the benzo-bis(thiadiazole)—thiophene copolymer, where the codimer have absorption maxima at 702 nm (1.7 eV) [27,29] and the polymer have absorption maxima at 902 nm (1.3 eV) [25].

The substitution in different positions also shows a large effect on the band gap [30]. It was shown for dodecyl side chains that having the side chain close to the benzothiadiazole ring in position 3 on thiophene compared to the 4 position causes the band gap to increase due to steric hindrance, which causes the planarity to break [30]. However, for the polymer with the alkyl chain in the 4 position the band gap was increased when the alkyl chain was added compared to the insoluble analog with no side chains from 1.1 to 1.96 eV [30]. The use of alkyl side chains was of great importance to insure solubility of the polymer [25]. Several alkyl chains have been tested, i.e. hexyl, 2-ethylhexyl, dodecyl and 3,7,11-trimethyldodecyl. It was

found that the latter gave the best film formability [25]. The use of four alkoxy groups on the two thiophene units (Fig. 28) resulted in a soluble polymer with a band gap of 1.72 eV in solution and 1.55 eV in solid state [191].

The synthesis of the copolymers has been carried out by three different methods as shown in Fig. 30.

(1) Stille cross-coupling polymerization of di-stannyl derivatives of thiophene or di-thiophenes and di-bromo derivatives of benzothiadiazole or benzo-bis(thiadiazole) with a Pd catalyst [25,190].
(2) Oxidative ferric chloride polymerization of the monomer with a FeCl$_3$ catalyst [25,190].
(3) Polymerization of the di-brominated monomers with Ni(COD)$_2$ as a catalyst in a Yamamoto coupling [191].

The polymer based on benzothiadiazole and two thiophenes have been synthesized with both alkyl [25,190] and alkoxy groups [191] to give soluble polymers. The synthesis was carried out by oxidative ferric chloride polymerization for the alkyl [25,190] and by Yamamoto coupling polymerization for the polymer with alkoxy
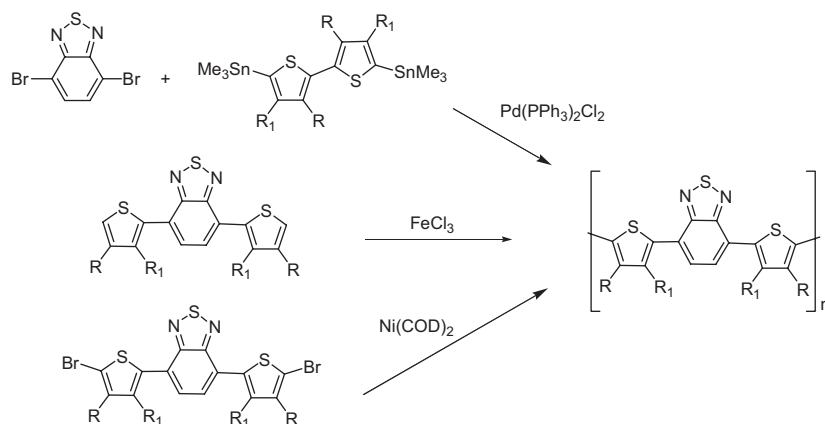
Fig. 30. Synthesis of copolymers based on thiophene and benzothiadiazole or benzobisthiadiazole by Stille, ferric or Yamamoto [25,189–191].
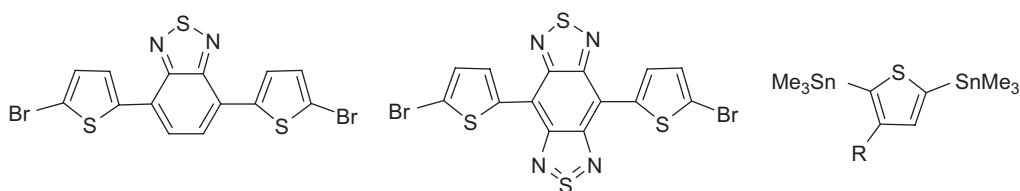

Fig. 31. Other building blocks for Stille cross-coupling polymerization which will result in the copolymers shown in Fig. 28 [25].

Table 6
Photovoltaic responses obtained for copolymers based on benzothiadiazole and thiophene

Polymer	Polymer/ PCBM	Area (cm^2)	Annealing temperature (°C)	I_{SC} (mA cm^{-2})	V_{OC} (V)	FF (%)	η (%)	IPCE/λ (%, nm)	Notes	Refs.
PTBT(OR)	1:4	0.1–0.15	—	3.4	0.77	42	0.9	13/650	LiF/Al, 75 mW cm^{-2}	[191]
PTBT(HH)	1:1	3	70 (2 min)	0.02	0.61	24	0.02	0.6/450		[190]
PTBT(HT)	1:1	3	No	0.03	0.33	30	0.02	—		[190]
PTTBTT	1:2	3	70 (10 min)	2.70	0.58	38	0.6	22/560		[26]
PTTBTT	1:2	10	70 (10 min)	1.29	0.56	28	0.2	—		[26]
PTTBTT	1:2	0.1	110 (10 min)	3.59	0.61	46	1.0	18/600	100 mW cm^{-2}	[192]

The measurements were carried out at 1000 Wm^{-2} and AM1.5 unless otherwise noted. The structure of the devices was: ITO/PEDOT:PSS/pol:PCBM/ LiF/Al.

groups [191]. Part of the polymers shown in Fig. 28 was synthesized by Stille cross coupling between other building blocks, which are shown in Fig. 31 [25].

The copolymer based on di-thiophene and benzo-bis(thiadiazole) have also been synthesized from the monomer by a potential sweep electrolysis in an argon degassed PhCN solution with nBu$_4$NBF$_4$ [27,29].

The CV diagrams for benzothiadiazole and benzo-bis(thiadiazole) showed that the n-doping process was sharp and quasi-reversible and the p-doping was broad and irreversible [27]. Further, the benzo-bis(thiadiazole) showed a low degree of n-doping charge before the main reduction peak [27]. This was ascribed to charge trapping in the benzo-bis(thiadiazole) unit [27].

Only a few examples of application of these polymers in OPVs have been reported and the results are summarized in Table 6 [26,190–192]. Different effects have been shown to influence the performance of the OPV devices. The morphology and hence the performance of OPV devices with the copolymer based on benzothiadiazole and four thiophenes was found to depend on solvent choice, spin rate, concentration of the spin coated solution and annealing temperature of the device where efficiencies of up to 1% was reported [192].

The regioregularity of the alkyl substituents (hexyl) was found to have a small effect on the PV responses [190]. The head-to-head coupled polymer gave a higher efficiency when applied in OPV devices (as a homopolymer) when compared to the head-to-tail coupled copolymer. However, when used in bulk heterojunctions with PCBM the polymers gave the same efficiency after the head-to-head coupled polymer was annealed [190].

Lifetime studies on these types of low band gap polymers are severely limited, however, an increase in lifetime have been reported when bilayer devices were prepared with C_{60} and a copolymer of thiophene and benzothiadiazole with four thiophenes in the repeating unit [26]. An increase from 2 to 80 h was observed when comparing to a device prepared with the homopolymer [26].
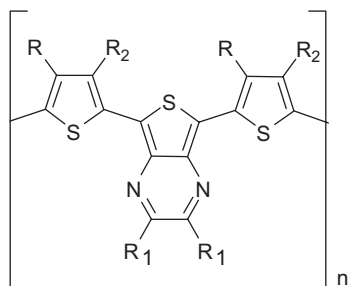

Fig. 32. Structure of thienopyrazine in a copolymer with thiophene. PB3OTP, $R_2 = C_8H_{17}$ [193], PTBEHT: $R = R_2 = H$, $R' =$ phenyl-2-ehtylhexyloxy and PBEHTT: $R' = H$, $R =$ phenyl-2-ehtylhexyloxy [194].
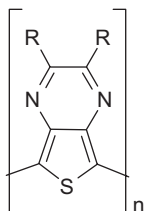
Fig. 33. Structure of poly(thienopyrazine) [195].

3.7. Copolymers based on thienopyranozine (PTP)

The copolymer based on thienopyranozine and thiophene is another example of the alternation between aromatic and quinoid units, which results in a low band gap polymer. Here thiophene is again used as the electron donor and thienopyranozine is used as the electron acceptor. The thienopyranozine is a thiophene with a fully fused aromatic pyrazine ring in position 3 and 4, and is thus similar in construction to ITN as shown in Fig. 32.

The synthesis of the homopolymer of thienopyrazine (Fig. 33) was first carried out by an oxidative ferric polymerization in chloroform [195] or from 2,3-pyrazine-dicarboxylic anhydride using P_4S_{10} [161]. The band gap of the polymer was found to be 0.95 eV (solid state) and the conductivity was found to be $3.6 \times 10^{-2}\,S\,cm^{-1}$ [195]. The polymer was also prepared with different alkyl side chains and polymerized electrochemically [196].

A few years later the copolymer based on thienopyrazine and thiophene was synthesized by electrochemical reduction of the monomer onto an ITO electrode in PhCN using Bu_4NClO_4 as catalyst [36] and the band gap was determined to be 1.0 eV [36]. The electrochemical polymerization was also carried out by a repetitive potential-sweep anodic oxidation with nBu_4NClO_4 in MeCN [27]. However, the result of this polymerization was an insoluble polymer regardless of the choice of side chains on the pyrazine ring.

The chemical synthesis of PTP has been carried out by two different methods as shown in Fig. 34.

(1) Oxidative ferric chloride polymerization of TP with dodecyl side chains [193].
(2) Polymerization of the dibrominated monomers with $Ni(COD)_2$ as a catalyst in a Yamamoto coupling [194].
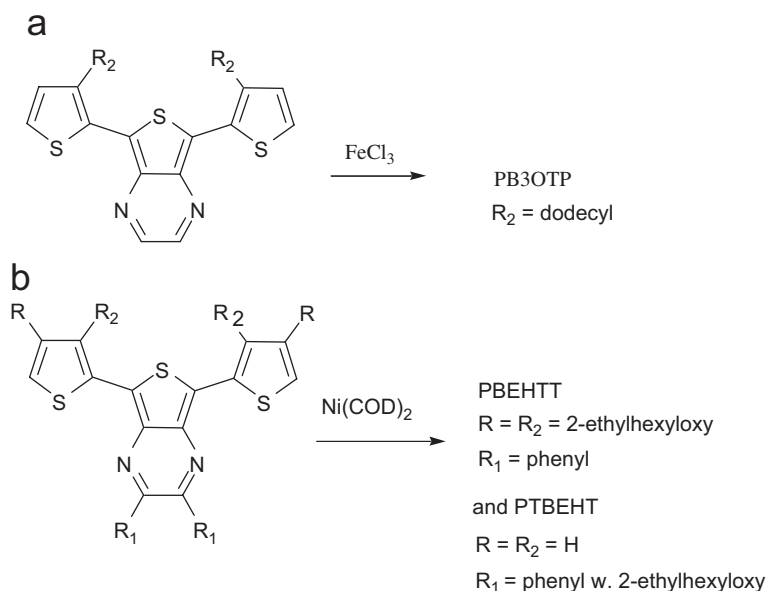

Fig. 34. Synthesis of copolymer of thienopyrazine and thiophene by (a) an oxidative ferric polymerization [193] and (b) a Yamamoto coupling polymerization [194,197].
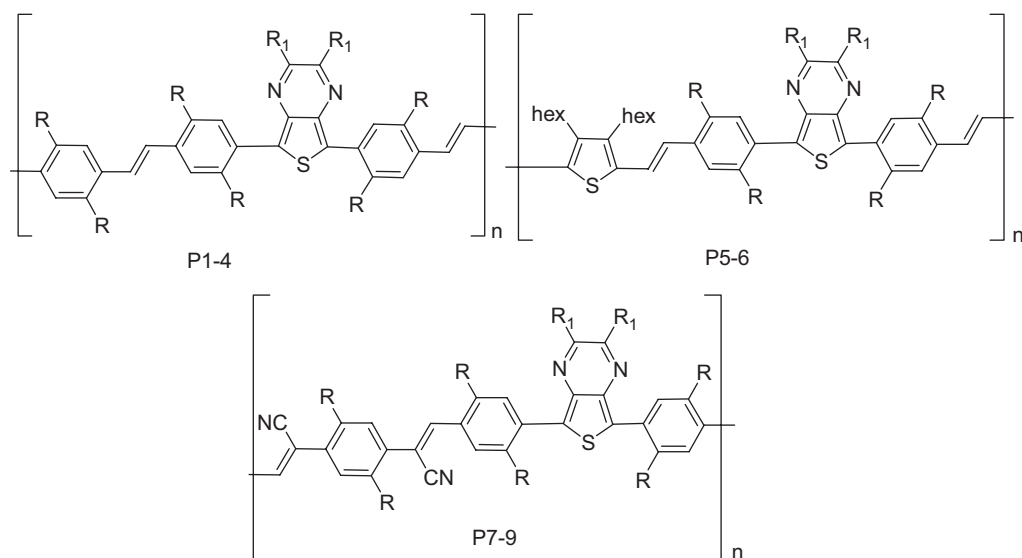
Fig. 35. Structures of copolymers of thienopyrazine and different vinyl-phenyl units.

Table 7
Photovoltaic responses obtained for copolymers based on thienopyrazine and thiophene

Polymer	Polymer/ PCBM	Area (cm^2)	Annealing temperature (°C)	I_{SC} (mA cm^{-2})	V_{OC} (V)	FF (%)	η (%)	IPCE/λ (%, nm)	Notes	Refs.
PB3OTP	1:1	0.05	—	1.0	0.22	39	—	6/660	$100\,mW\,cm^{-2}$	[193]
PBEHT	1:4	0.15	—	1.3	0.39	57	0.29	2/800		[194]
PTBEHT	1:4	0.15	—	3.5	0.56	58	1.1	10/800		[194]

The measurements were carried out at $75\,mW\,cm^{-2}$ and AM1.5 unless otherwise noted. The structure of the devices was: ITO/PEDOT:PSS/pol:PCBM/LiF/Al.

The band gap of the polymers was found to be 1.3 eV for PB3OTP [193], 1.20 eV for PTBEHT [194] and 1.28 eV for PBEHTT [194]. The lower band gap of PTBEHT compared to PBEHTT is ascribed to the improved conjugation and more coplanar structure of PTBEHT caused by the absence of bulky substituents [194]. PB3OTP showed a broad absorption range 300–980 nm with a maximum at 730 nm [193].

The polymers shown in Fig. 35 were prepared by Horner (P1–P6) or Knoevenagel (P6–P9) polycondensation. The polymers showed band gaps of 1.56–2.08 eV (1.56 eV for P6 $R_1 = O$-hexyl) [198].

The OPV devices prepared with PTP showed different responses depending on the side chains. The results are summarized in Table 7. The optimum ratio between the polymer and PCBM was different for the three polymers, i.e. 1:1 for PB3OTP [193] and 1:4 for PBEHTT and PTBEHT [194].

AFM images of PBEHTT showed a rough surface and phase separation, and for PTBEHT the AFM images showed a smooth surface with a more intimate mixing of the polymer and PCBM and thus a higher efficiency for PTBEHT was observed [194]. From Table 7 it can be seen that the reduction in band gap from 1.9 eV for P3HT to

1.2 eV for PTBEHT causes only a small change in V_{OC} [194]. The poor efficiency of the OPVs with PB3OTP was ascribed to the low V_{OC} [193].

3.8. Copolymers based on polyfluorene

The homopolymer of polyfluorene have a large band gap (3.68 eV) and have been used as a blue light emitter in light-emitting diodes [199–202]. However, the light emitted and hence the band gap of polyfluorene could be tuned with addition of different electron donating or electron accepting units in the back bone of the polymer [201]. Within the past few years the focus on fluorene units incorporated in alternating donor acceptor polymers have therefore increased tremendously.

3.8.1. Copolymers based on thiophene, benzothiadiazole and fluorene

The copolymer based on thiophene, benzothiadiazole and fluorene (Fig. 36) is an example of the alternation of the electron donating unit, thiophene/fluorene, and the electron accepting unit, benzothiadiazole.

The synthesis of the copolymer based on thiophene, benzothiadiazole and fluorene was carried out by Suzuki

cross-coupling with Pd as catalyst as shown in Fig. 37.1 [201]. This polymerization was also carried out without the di-bromofluorene derivative as a comonomer as shown in Fig. 37.2 [203].

The band gap of the copolymer was estimated from UV-vis to be 2.01 eV. [201,203] Hou et al. found that due to exciton trapping in the benzothiadiazole unit efficient charge transfer was achieved [201].

A derivative of the polymer shown in Fig. 36 was prepared with O-alkyl side chains on the thiophene rings, PF-co-DTB [204]. The polymer was synthesized by a Suzuki coupling shown in Fig. 37 [204] and the band gap was found to be 1.78 eV [204].

A selenium derivative of the copolymer (Se instead of S in the thiadiazole ring) has also been prepared by Suzuki cross coupling and had a band gap of 1.87 eV [205].

The derivative shown in Fig. 38 was synthesized by the routes shown in Fig. 37 and applied in OPV devices [206].

Several groups have studied OPV devices and the results are summarized in Table 8.

For the device in entry 4 of Table 8 morphological studies were carried out with different solvent systems, i.e. CHCl$_3$ or CHCl$_3$ mixed with xylene, toluene or chlorobenzene. It was found that V_{OC} was constant but I_{SC} varies with the solvent system [210]. The highest I_{SC} was achieved for the CHCl$_3$ and chlorobenzene mixture (data given in Table 8). AFM images of the film showed a more

fine and uniform distribution of domains (RMS = 1.1–1.2) [210]. Investigations of the PCBM content showed a maximal efficiency for 20–50% w/w PCBM content, however, the highest I_{SC} was obtained with 80% w/w PCBM content [218]. It was shown by time-resolved spectroscopy that the performance of the OPV is limited by charge transport and not formation of charges [219]. A detailed review of the use of the copolymers based on PFO and benzothiadiazole in PLED was published in 2000 by Bernius et al. [199].

3.8.2. Copolymers based on thienopyrazine or thiadiazolequinoxaline, thiophene and polyfluorene

The copolymer based on thiophene, fluorene and thieno-pyrazine or thiadiazolequinoxaline as shown in Fig. 39 is another example of the alternation of the electron donating unit, thiophene/fluorene, and the electron accepting unit, thienopyrazine or thiadiazolequinoxaline.

The copolymers were also synthesized by a Suzuki polymerization as shown in Fig. 37 [27,203]. The reported band gaps for APFOGreen1, 2, 3 and 4 was 1.27 eV [35,216,218,220], 2 eV [215], 1.4 and 1.3 eV [217], respectively. The reported λ_{max} was at 400 and 780 nm for APFOGreen1 [35,216,220] and at 780 and 740 nm for APFOGreen3 and 4 [217], respectively. Further, APFO-Green1 was found to have a high field effect mobility of 0.03 cm^2 V^{-1} s^{-1} [221].

The polymers have been applied in OPV devices and the results are summarized in Table 8. It was found that the charge separation in the devices with these polymers was better when BTPF70 (Fig. 40) was used as electron acceptor compared to devices prepared with PCBM as electron acceptor, due to the higher LUMO level of BTPF70, and hence the better contact with the LUMO level of the polymer [209,214]. Studies on APFO-Green1 in blends with PCBM and BTPF70 showed that the hole mobility has maximum at 67 wt% PCBM and decreases
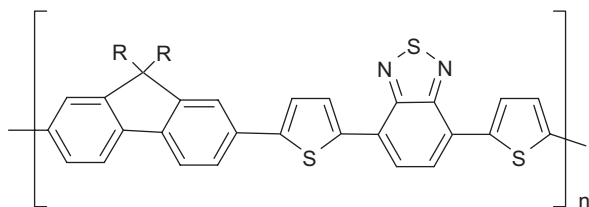

Fig. 36. Copolymer based on benzothiadiazole, thiophene and fluorene, PFO-DTBT.
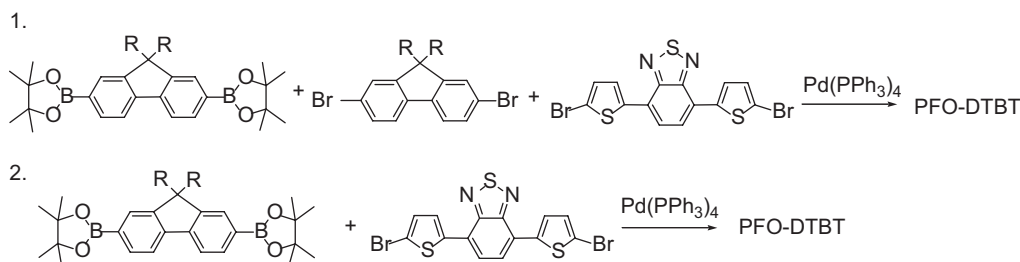

Fig. 37. Synthesis of copolymer based on benzothiadiazole, thiophene and fluorene, PFO-DTBT.
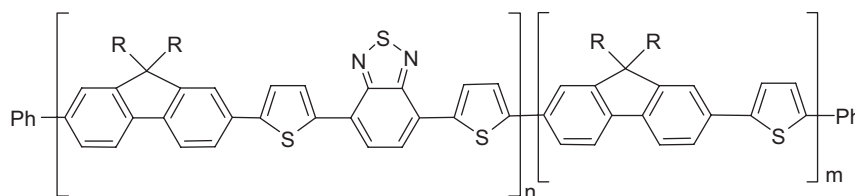

Fig. 38. APFOGreen 5 [206].

Table 8
Photovoltaic responses obtained for copolymers based on fluorenes

Polymer	Polymer/PCBM	Area (cm^2)	Annealing temperature (°C)	I_{SC} (mA cm^{-2})	V_{OC} (V)	FF (%)	η (%)	IPCE/λ (%, nm)	Notes	Refs.
PFDTBT	1:4	1.0	—	4.66	1.04	46	2.2	40/550		[203]
PFO-DBT35	1:2	—	—	5.18	0.95	35	2.24[a]	—	Ba/Al	[207]
PFO-DBT	1:4	0.04–0.06	—	3.55	1.01	58	2.1	45/550		[208,209]
PFO-DBT	1:3	0.04–0.05	—	4.6	1.03	49	2.3	45/550		[210]
Red B	1:3	—	95	2.4[b]	0.9	—	0.75[b]	—	Ca cathode, 75 mW cm^{-2}	[211]
Selene derivate	1:4	0.15	—	2.53	1.0	37	1.0	—	Ba/Al 78 mWcm^{-2}	[205]
PPV derivate	1:1 C$_{60}$	0.04	—	2.52–3.09	0.81–0.93	38–40	0.94–1.02	22/500	Ca cathode	[212]
APFOGreen1	1:4 BTPF70 (C$_{70}$)	0.04–0.06	—	3.4	0.58	35	0.7	28/400, 8.8/850, 7/900		[213]
APFOGreen1	1:4 BTPF (C$_{60}$)	0.04–0.06	—	1.76	0.54	32	0.3	22/400, 8.4/850, 7/900		[209,213,214]
APFOGreen2	1:4	0.04–0.06	—	3.0	0.78		0.9	10/650		[215,216]
APFOGreen3	1:4 BTPF70 (C$_{70}$)	0.04–0.06	—	2.4	0.61	40	0.59	8/800	1000 Wm^{-2}	[217]
APFOGreen4	1:4 BTPF70 (C$_{70}$)	0.04–0.06	—	2.1	0.56	30	0.37	6/800	1000 Wm^{-2}	[217]
LBPF3	1:4	—	—	3.1	1.07	51	1.7[c]	40/400–560		[206]
PF-co-DBT	1:4	0.11	—	4.31	0.76	48.6	1.60	23/575		[204]

The measurements were carried out at 100 mW cm^{-2} and AM1.5 unless otherwise noted. The structure of the devices was: ITO/PEDOT:PSS/pol:PCBM/LiF/Al.

[a]Measured at 78 mW cm^{-2}. I_{SC} increase linearly with increase in light intensity up to 500 mW cm^{-2} (5 sun).

[b]η and I_{SC} was found to depend on temperature and PCBM content.

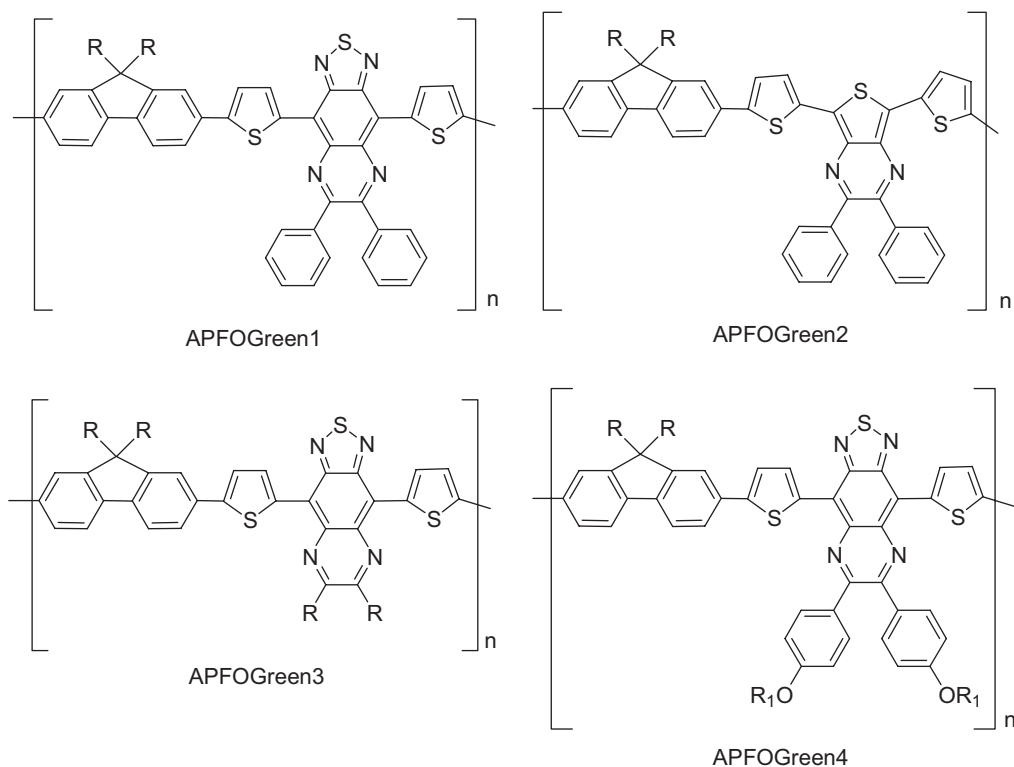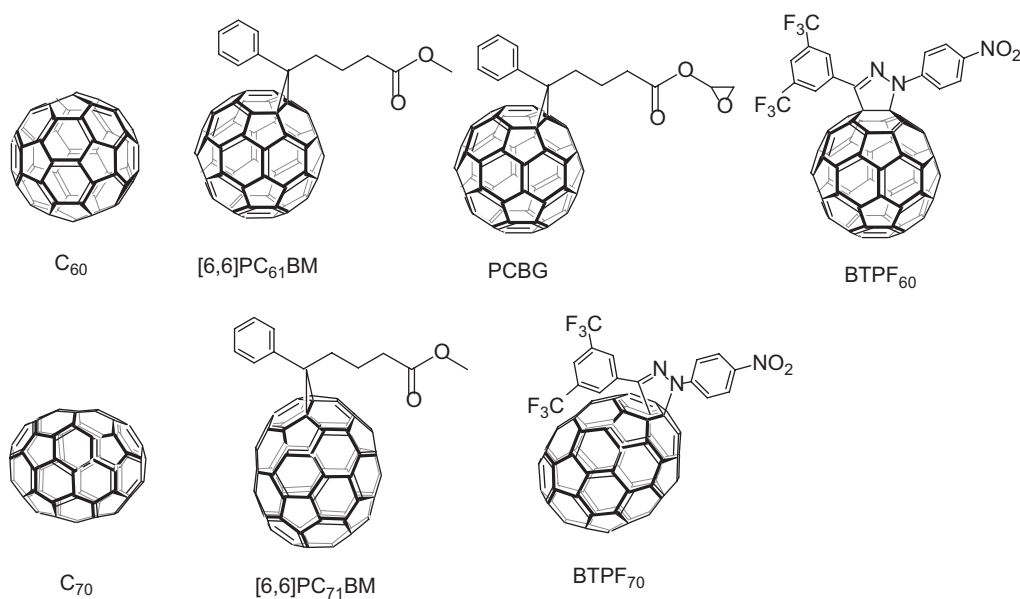[c]η and I_{SC} was found to depend on thickness and ratio of polymer and PCBM (thickness here 200 nm).

Fig. 39. APFOGreen 1, 2, 3 and 4 where R = alkyl [35,209,213–221].

Fig. 40. Structure of electron acceptors used in OPV devices: C_{60}, [6,6]-$PC_{61}BM$, PCBG [111], $BTPF_{60}$, C_{70}, [6,6]-$PC_{71}BM$ [223] and $BTPF_{70}$.

when more BTPF70 was added. The electron mobility increases with an increases in both cases when increasing the acceptor content. However, BTPF70 gives better exciton dissociation even though the structural inhomogenity yields poor charge transport [222].

A few other examples of copolymers based on fluorene and different aromatic units have been published [212,224,225]. The polymer shown in Fig. 41 had a band gap of 1.95 eV [225] and the OPV results are given in Table 8.
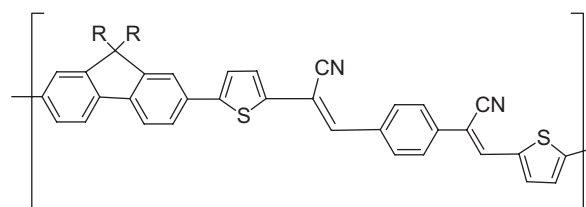
Fig. 41. Copolymer based on fluorine, thiophene and phenylvinyl (PFTPV) [225].

Table 9
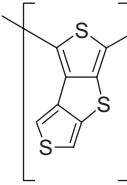Other low band gap polymers described in the literature
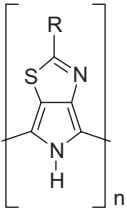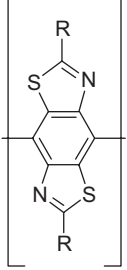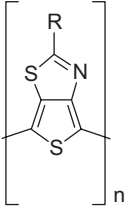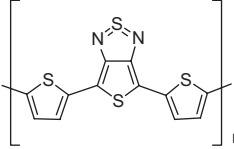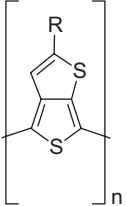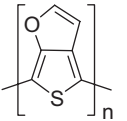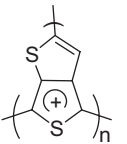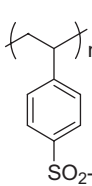
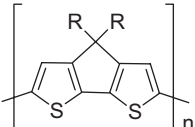| Structure	Band gap (λ_{max}) eV, nm	Polymerization	Refs.
	1.22–1.75 (575)	Oxidative ferric chloride ($FeCl_3$)	[226]
	2 (500)	Ullmann coupling (Cu) or reaction with Ni(0)	[227]
	1.26–1.30 (725)	Electrochemical	[228]
	1.1 (590)	Electrochemical	[229–232]
	0.9	Electrochemical, monomer synthesised from 3,4-diaminothiophene	[233,234]
	Solution: 0.98 (739) Film: 0.92 (925)	Oxidative ferric chloride ($FeCl_3$) or electrochemical	[235–240]
	1.03	Electrochemical	[241,242]
	>1.0	Oxidation from thieno-thiophene (PSSA)	[243,244]

Table 9 (continued)
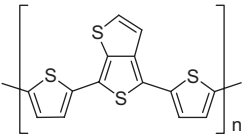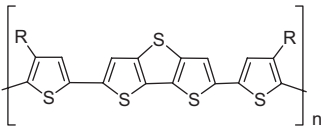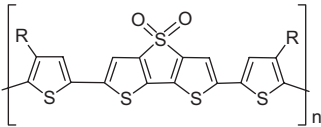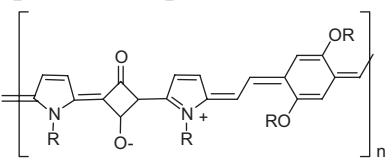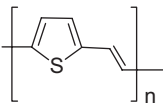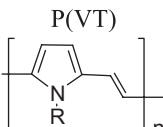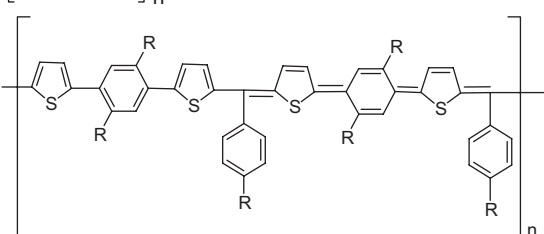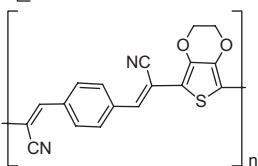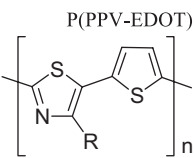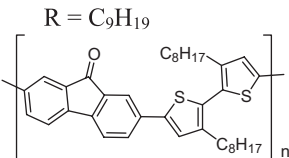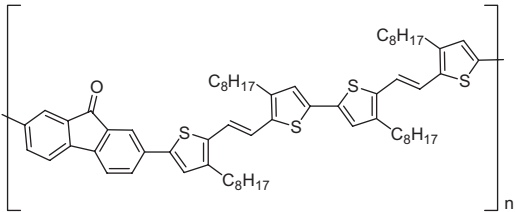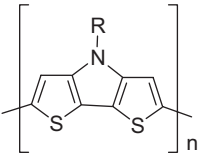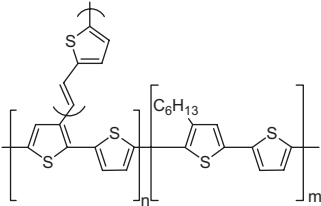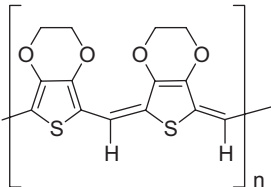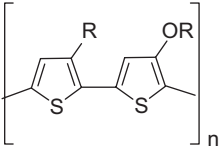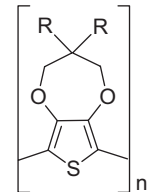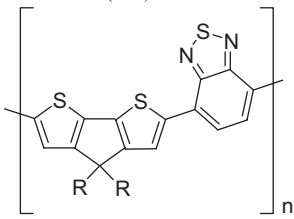
Structure	Band gap (λ_{max}) eV, nm	Polymerization	Refs.
	1.6	Electrochemical	[245]
	2.0	Suzuki coupling with DDT and distannyl derivative of alkyl-thiophenes	[246]
	1.7	Suzuki coupling with DDT-ox and distannyl derivative of alkyl-thiophenes	[246]
	1.8	Oxidative ferric chloride ($FeCl_3$)	[247]
	0.5	Acid-catalysed polycondensation	[37,248–251]
P(VT)	1.7–1.8	(1) base elimination (bis-sulfoxide monomer, (2) xanthate, (3) dicarbonate, (4) oxidative ferric chloride ($FeCl_3$)	[252–257]
	1.7	Bu^{t}OK	[252,258]
	1.0	Oxidative dehydrogenation w. DDQ	[259–262]
P(PPV-EDOT)	1.69	Oxidative ferric chloride ($FeCl_3$)	[263]
R = C_9H_{19}	1.8–2.0 (solution: 467, film: 520, 560 and 605)	Suzuki between di-bromo derivative of imidazole and di-stannyl of thiophene	[264]
PDOBTF	1.98	Oxidative ferric chloride ($FeCl_3$)	[265]

Table 9 (*continued*)

Structure	Band gap (λ_{max}) eV, nm	Polymerization	Refs.
 PTVF	1.52	Oxidative ferric chloride (FeCl$_3$)	[265]
	1.6–1.8	FeCl$_3$ or NOBF$_4$ or electrochemical	[92]
 3D-PT	1.99	Stille cross coupling	[117]
	$\leqslant 1$	Acid-promoted polycondensation	[266]
 POT-co-DOT	1.64 (solution: 538, film: 621)	Yamamoto	[204]
 PProDOT(Hx)$_2$	1.9	Grignard of di-bromo derivative (Ni(dppp)Cl$_2$)	[267,268]
 R = 2-ethylhexyl,PCPDTBT	1.73	–	[269,270]

4. Other low band gap polymers

In addition to the low band gap polymers described above other examples have been described in the literature. These are summarized in Table 9.

Only a few of these polymers have been applied in OPV devices, and the results for these are summarized in Table 10.

In 2005 Somez et al. reported a band gap of 0.7 eV for a copolymer of thiophene and thienopyrazine which was covalently bonded to C_{60} [271]. This polymer is not shown. In 2006, Cremer and Bäuerle reported on a star shaped dendrimer with an *N*-triphenyl core as donor and thiophene arms as acceptor. The band gap was varied with the length of the arms from 1.72 to 1.65 eV [272].

5. Impurities and doping

One currently unanswered question that remains for many of these materials is the extent of doping impurities that could affect the performance of PV devices prepared from them. Efficient methods have been reported and are commonly employed for the most studied materials today such as P3HT, MEHPPV and MDMOPPV. However, the low band gap materials that must still be considered as rather exotic materials are generally available in the few laboratories who has the experience to make them. Further, many of them are only available in small quantities and are unavailable to the public. Hopefully, many of these low band gap polymer materials will be made available in large quantities so that research groups that specialize in device preparation and testing can give their value for the efficiency that can be obtained for these materials. To this end it is very important to establish the level of impurities and if possible remove them. For instance the polymers described in Sections 3.3 and 3.4 could include impurities from $FeCl_3$, H_2SO_4 and PO_4^{2-} from the polymerization reaction and there are no well documented efforts that deal with removal and estimation of the residual amount of impurities nor any correlation with the influence impurities may have on PV device

operation. In Sections 3.5–3.8 polymerization is exclusively achieved with transition metal catalysts such as palladium and nickel and these are notoriously included in the polymer product as nanoparticles [273]. Very efficient methods for removal of the transition metal impurities have been developed and reported for both polymer products [274] and small molecule intermediates [275]. This has been used for purification and analysis in a few instances [25,85,276]. There has been only one other example that documents removal of nickel from a Yamamoto coupling using EDTA [194] and in general the level of transition metal impurities in products obtained by these reactions must be expected to be significant, especially in cases where the purification procedure is not described or mentioned. Finally the electron-rich low band gap materials with a high HOMO level can arguably be doped by molecular oxygen. This has been observed for thin film transistor devices where the influence of doping by molecular oxygen is observed in field effect mobility measurements. The removal of doping impurities that could stem from oxygen or from oxidation by molecular oxygen in the presence of a suitable anion has been investigated in the supplementary section of one literature report [25] by treatment with hydrazine and ammonia albeit with little change in the resulting properties.

6. Chemical stability

Chemical stability and degradation of polymers in OPV devices is of great importance, however, to our knowledge only a few reports on the issue have been published. For the low band gap polymers described above the studies are limited to a report on a P3HT/PCBM device [116], a copolymer based on thiophene and benzothiadiazole [26] and a polythiophene with thermocleavable side chains which have an estimated lifetime of 20,000 h under normal operating conditions [9]. Studies of the degradation mechanisms in OPVs have shown that the mechanisms include reaction with oxygen and water in the atmosphere and with the electrode materials. However, the mechanisms are complicated and hence only few reports dedicated to an

Table 10
OPV devices with other low band gap polymers

Polymer	Polymer/PCBM	I_{SC} (mA cm^{-2})	V_{OC} (V)	FF (%)	η (%)	IPCE at λ (%, nm)	Notes	Refs.
3D-PT	1:1	10.3	0.72	43	3.18	60/450–550	Mg/Al	[117]
POT-α-DOT	1:1	0.22	0.60	41.2	0.054	—		[204]
P(PPV-EDOT)	1:1	0.73	0.28	28	—	—		[263]
P(VT)	1:2	3.50	0.35	50	0.6	17/550		[256]
PDOBTF	1.26 molar eq	0.77	0.34	28	0.09	10/430		[265]
PTVF	1.26 molar eq	2.97	0.5	58	1.1	21/420		[265]
PProDOT(Hx)$_2$	1:4	1.05	0.29	38	0.1	7.4/445		[268]
PCPDTBT	—	9	0.65–0.70[a]	47[a]	2.67	25–35/400–800[a]		[269,270]
PCPDTBT	-(PC$_{71}$BM)	11	0.65–070[a]	47[a]	3.16	38/700		[269,270]]

The measurements were carried out at 100 mW cm^{-2} and AM1.5 unless otherwise noted. The structure of the devices was: ITO/PEDOT:PSS/pol:PCBM/LiF/Al.
[a]Values not unambiguously quoted in Ref. [269].

understanding of the mechanism have been published [277–282]. Future applications of OPVs rely heavily on the understanding of the degradation phenomena and on the development of new materials and efficient encapsulation of the OPV and alternative barrier layers which are more impervious to oxygen and water from the atmosphere.

7. Conclusion

The spectrum of the sun as received on earth has been presented in the context of light harvesting by low band gap polymer materials and an evaluation of the possible currents that can be obtained for a material with a given band gap has been considered. The existing literature on polymer materials with a band gap below 2 eV have been examined and discussed in the context of polymer PV devices. The field of low band gap polymer materials for OPV is concluded to be emerging. The current problems that one is faced with when considering the application of low band gap materials are the achievement of simple large scale synthetic quantities of materials that are sufficiently pure for incorporation in devices. Further, high values for the IPCE has been reported for a few low band gap materials while the general observation is very low IPCE values that currently has been linked to carrier transport problems, perhaps impurities, poor film forming ability of the materials and a low solubility making processing difficult. Methods for purifying the materials from impurities are reported in a few instances and are deemed important for future reproducibility of results obtained for the same class of materials. The field is increasing and the success of the low band gap approach will be granted through: large-scale synthetic approaches, availability in large quantities, purification and purity, widespread physical studies and optimization.

Acknowledgments

References

[1] H. Spanggaard, F.C. Krebs, Sol. Energy Mater. Sol. Cells 83 (2004) 125.
[2] Organic-based photovoltaic, MRS Bull. Special Issue 5 (2005) 1.
[3] B. Maennig, J. Drechsel, D. Gebeyehu, P. Simon, F. Kozlowski, A. Werner, F. Li, S. Grundmann, S. Sonntag, M. Koch, K. Leo, M. Pfeiffer, H. Hoppe, D. Meissner, N.S. Sariciftci, I. Riedel, V. Dyakonov, J. Parisi, Appl. Phys. A 79 (2004) 1.
[4] H. Hoppe, N.S. Sariciftci, J. Mater. Rev. 19 (2004) 1924.
[5] C.J. Brabec, Sol. Energy Mater. Sol. Cells 83 (2004) 273.
[6] C. Winder, N.S. Sariciftci, J. Mater. Chem. 14 (2004) 1077.
[7] C.J. Brabec, S.E. Shaheen, T. Fromherz, F. Padinger, J.C. Hummelen, A. Dhanabalan, R.A.J. Janssen, N.S. Sariciftci, Synth. Met. 121 (2001) 1517.
[8] S.-S. Sun, N.S. Sariciftci, Organic Photvoltaics—Mechanisms, Materials, Devices, CRC Press, Boca Raton, FL, ISBN 0-8247-5963-X, 2005.
[9] F.C. Krebs, H. Spanggaard, Chem. Mater. 17 (2005) 5235.
[10] M. Reyes-Reyes, K. Kim, J. Dewald, R. López-Sandoval, A. Avadhanula, S. Curran, D.L. Carroll, Org. Lett. 7 (2005) 5749.
[11] W. Ma, C. Yang, X. Gong, K. Lee, A.J. Heeger, Adv. Funct. Mater. 15 (2005) 1617.
[12] R. Gaudiana, R. Eckert, J. Cardone, J. Ryan, A. Montello, Proc. SPIE 6334 (2006) 633401.
[13] H. Hoppe, N.S. Sariciftci, J. Mater. Chem. 16 (2006) 45.
[14] J. Roncali, Chem. Rev. 97 (1997) 173.
[15] T.A. Skotheim, R.L. Elsenbaumer, J.R. Reynolds, Handbook of Conducting Polymers, second ed, Marcel Dekker, New York, 1998, pp. 225–309, ISBN0-8247-0050-3.
[16] A.K. Bakhshi, G. Bhalla, J. Sci. Ind. Res. 63 (2004) 715.
[17] A. Dhanabalan, J.K.J. van Duren, P.A. van Hal, J.L.J. van Dogen, R.A.J. Janssen, Adv. Funct. Mater. 11 (2001) 255.
[18] J.K.J. van Duren, A. Dhanabalan, P.A. van Hal, R.A.J. Janssen, Synth. Met. 121 (2001) 1587.
[19] H. Neugebauer, C.J. Brabec, N.S. Sariciftci, R. Kiebooms, F. Wudl, S. Luzzati, J. Chem. Phys. 110 (1999) 12108.
[20] National Renewable Energy Laboratory (NREL), MS Excel^{TM} spreadsheet file downloaded from ⟨http://rredc.nrel.gov/solar/spectra/am1.5/⟩.
[21] M.C. Scharber, D. Mühlbacher, M. Koppe, P. Denk, C. Waldauf, A.J. Heeger, C.J. Brabec, Adv. Mater. 18 (2006) 789.
[22] L.J.A. Koster, V.D. Mihailetchi, P.W.M. Blom, Appl. Phys. Lett. 88 (2006) 093511.
[23] K.M. Coakley, M.D. McGehee, Chem. Mater. 16 (2004) 4533.
[24] M. Jørgensen, F.C. Krebs, Pol. Bull. 51 (2003) 23.
[25] E. Bundgaard, F.C. Krebs, Macromolecules 39 (2006) 2823.
[26] E. Bundgaard, F.C. Krebs, Sol. Energy Mater. Sol. Cells 91 (2007) 1019–1025, this issue; doi:10.1016/j.solmat.2007.01.13.
[27] C. Kitamura, S. Tanaka, Y. Yamashita, Chem. Mater. 8 (1996) 570.
[28] J.L. Brédas, A.J. Heeger, F. Wudl, J. Chem. Phys. 85 (1986) 4673.
[29] M. Karikomi, C. Kitamura, S. Tanaka, Y. Yamashita, J. Am. Chem. Soc. 117 (1995) 6791.
[30] M. Jayakannan, P.A. van Hal, R.A.J. Janssen, J. Pol. Sci. A Pol. Chem 40 (2002) 251.
[31] K.G. Jespersen, W.J.D. Beenken, Y. Zaushitsyn, A. Yartsev, M. Andersson, T. Pullerits, V. Sundström, J. Chem. Phys. 121 (2004) 12613.
[32] K.G. Jespersen, A. Yartsev, T. Pascher, V. Sundström, Synth. Met. 155 (2005) 262.
[33] N.-K. Persson, M. Sun, J. Chem. Phys. 123 (2005) 204718 1-9.
[34] L. Yang, J.-K. Feng, A.-M. Ren, Polymer 46 (2005) 10970.
[35] M. Chen, E. Perzon, M.R. Andersson, S. Marcinkevicius, S.K.M. Jönsson, M. Fahlman, M. Berggren, Appl. Phys. Lett. 84 (2004) 3570.
[36] C. Kitamura, S. Tanaka, Y. Yamashita, J. Chem. Soc. Chem. Commun. (1994) 1585.
[37] A. Ajayaghosh, Chem. Soc. Rev. 32 (2003) 181.
[38] S.C. Rasmussen, B.D. Straw, J.E. Hutchison, Semiconducting polymers applications properties and synthesis, in: B.R. Hsieh, Y. Wei (Eds.), ACS Symposium Series 735, American Chemical Society, Washington, DC, 1999, pp. 347–366, ISBN0-8412-3612-7.
[39] P. Schilinsky, U. Asawapirom, U. Scherf, M. Biele, C.J. Brabec, Chem. Mater. 17 (2005) 2175.
[40] D.W. Breiby, E.J. Samuelsen, O. Konovalov, Synth. Met. 139 (2003) 361.
[41] D.W. Breiby, E.J. Samuelsen, J. Pol. Sci. B: Pol. Phys. 41 (2003) 2375.
[42] K.E. Aasmundtveit, E.J. Samuelsen, M. Guldstein, C. Steinsland, O. Flornes, C. Fagermo, T.M. Seeberg, L.A.A. Pettersson, O. Inganäs, R. Feidenhans'l, S. Ferrer, Macromolecules 33 (2000) 3120.

[43] K.E. Aasmundtveit, E.J. Samuelsen, W. Mammo, M. Svensson, M.R. Andersson, L.A.A. Pettersson, O. Inganäs, Macromolecules 33 (2000) 5481.

[44] D. Fichou, J. Mater. Chem. 10 (2000) 571.

[45] H.J. Fell, E.J. Samuelsen, M.R. Andersson, J. Als-Nielsen, G. Grübel, J. Mårdalen, Synth. Met. 73 (1995) 279.

[46] H.J. Fell, E.J. Samuelsen, J. Mårdalen, M.R. Andersson, Synth. Met. 69 (1995) 283.

[47] J. Mårdalen, E.J. Samuelsen, Synth. Met. 48 (1992) 363.

[48] T.J. Prosa, M.J. Winokur, J. Moulton, P. Smith, A.J. Heeger, Macromolecules 25 (1992) 4364.

[49] L. Sicot, C. Fiorini, A. Lorin, P. Raimond, C. Sentein, J.-M. Nunzi, Sol. Energy Mater. Sol. Cells 63 (2000) 49.

[50] J. Nakamura, K. Murata, K. Takahashi, Appl. Phys. Lett. 87 (2005) 132105 1-3.

[51] J. Huang, G. Li, Y. Yang, Appl. Phys. Lett. 87 (2005) 112105 1-3.

[52] A.J. Mozer, N.S. Sariciftci, A. Pivrikas, R. Österbacka, G. Juška, L. Brassat, H. Bässler, Phys. Rev. B 71 (2005) 035214 1 9.

[53] R.J. Kline, M.D. McGehee, E.N. Kadnikova, J. Liu, J.M.J. Fréchet, M.F. Toney, Macromolecules 38 (2005) 3312.

[54] K. Sivula, C.K. Luscombe, B.C. Tompson, J.M. Fréchet, J. Am. Chem. Soc. 128 (2006) 13988.

[55] M.R. Andersson, O. Thomas, W. Mammo, M. Svensson, M. Theander, O. Inganäs, J. Mater. Chem. 9 (1999) 1933.

[56] U. Salzner, J.B. Lagowski, P.G. Pickup, R.A. Poirier, Synth. Met. 96 (1998) 177.

[57] R.D. McCullough, Adv. Mater. 10 (1998) 93.

[58] K.E. Aasmundtveit, E.J. Samuelsen, J. Mårdalen, E. Bakken, P.H.J. Carlsen, U. Lienert, Synth. Met. 89 (1997) 203.

[59] K.E. Aasmundtveit, E.J. Samuelsen, K. Hoffmann, E. Bakken, P.H.J. Carlsen, Synth. Met. 113 (2000) 7.

[60] E. Zhou, Z. Tan, C. Yang, Y. Li, Macromol. Rapid Commun. 27 (2006) 793.

[61] T. Yamamoto, K. Sanechika, A. Yamamoto, J. Pol. Sci. Pol. Lett. Ed. 18 (1980) 9.

[62] J.W.P. Lin, L.P. Dudek, J. Pol. Sci. Pol. Lett. Ed. 18 (1980) 2869.

[63] M. Sato, S. Tanaka, K. Kaeriyama, J. Chem. Soc. Chem. Commun. 11 (1986) 873.

[64] K.-Y. Jen, G.G. Miller, R.L. Elsenbaumer, J. Chem. Soc. Chem. Commun. 17 (1986) 1346.

[65] R.L. Elsenbaumer, K.Y. Jen, R. Oboodi, Synth. Met. 15 (1986) 169.

[66] R.D. McCullough, R.D. Lowe, M. Jayaraman, D.L. Anderson, J. Org. Chem. 58 (1993) 904.

[67] T.-A. Chen, R.D. Reike, J. Am. Chem. Soc. 114 (1992) 10087.

[68] R.D. McCullough, R.D. Lowe, J. Chem. Soc. Chem. Commun. (1992) 70.

[69] C. van Pharm, H.B. Mark Jr., H. Zimmer, Synth. Commun. 16 (1986) 689.

[70] D.D. Cunningham, L. Laguren-Davidson, H.B. Mark Jr., C. van Pharm, H. Zimmer, J. Chem. Soc. Chem. Commun. (1987) 1021.

[71] G. Consiglio, S. Gronowitz, A.-B. Hornfeldt, B. Maltesson, R. Noto, D. Spinelli, Chem. Scr. 11 (1977) 175.

[72] K. Tamao, K. Sumitani, Y. Kiso, M. Zembayashi, A. Fujioka, S. Kodama, I. Nakajima, A. Minato, M. Kumada, Bull. Chem. Soc. Japan 49 (1976) 1958.

[73] S. Kodama, I. Naajima, M. Kumada, A. Minato, K. Suzuki, Tetrahedron 38 (1982) 3347.

[74] R.D. McCullough, R.D. Lowe, Polym. Prep. 33 (1992) 195.

[75] R.D. McCullough, R.D. Lowe, M. Jayaraman, P.C. Ewbank, D.L. Anderson, S. Tristan-Nagle, Synth. Met. 55 (1993) 1198.

[76] R.D. McCullough, S. Tristan-Nagle, S.P. Williams, R.D. Lowe, M. Jayaraman, J. Am. Chem. Soc. 115 (1993) 4910.

[77] R.D. McCullough, S.P. Williams, S. Tristan-Nagle, M. Jayaraman, P.C. Ewbank, L. Miller, Synth. Met. 69 (1995) 279.

[78] K. Tamoa, K. Sumitani, M. Kumada, J. Am. Chem. Soc. 94 (1972) 4376.

[79] R.D. McCullough, J.A. Belot, S.P. Willams, Molecular engineering of advanced materials, in: J. Becher, K. Schaumburg (Eds.), NATO Adv. Res. Workshop Series, Series C: Math. and Phys. Sci., Kluwer, Dordrecht, vol. 456, 1995, pp. 349–363.

[80] R.D. McCullough, S.P. Willams, M. Jayaraman, J. Reddinger, L. Miller, S. Tristram-Nagle, Mater. Res. Soc. Symp. Proc. 328 (1994) 215.

[81] T.-A. Chen, R.D. Reike, Synth. Met. 60 (1993) 175.

[82] X. Wu, T.-A. Chen, R.D. Reike, Macromolecules 28 (1995) 2101.

[83] T.-A. Chen, X. Wu, R.D. Reike, J. Am. Chem. Soc. 117 (1995) 233.

[84] T.-A. Chen, R.A. O'Brien, R.D. Reike, Macromolecules 26 (1993) 3462.

[85] F.C. Krebs, M. Biancardo, Sol. Energy Mater. Sol. Cells 90 (2006) 142.

[86] A. Iraqi, G.W. Baker, J. Mater. Chem. 8 (1998) 25.

[87] J.M. Tour, Chem. Rev. 96 (1996) 537.

[88] Q.T. Zhang, J.M. Tour, J. Am. Chem. Soc. 119 (1997) 5065.

[89] S. Luzzati, M. Scharber, M. Catellani, F. Giacalone, J.L. Segura, N. Martin, H. Neugebauer, N.S. Sariciftci, J. Phys. Chem. B 110 (2006) 5351.

[90] J. Hou, L. Huo, C. He, C. Yang, Y. Li, Macromolecules 39 (2006) 594.

[91] E.E. Sheina, S.M. Khersonsky, E.G. Jones, R.D. McCullough, Chem. Mater. 17 (2005) 3317.

[92] K. Ogawa, J.A. Stafford, S.D. Rothstein, D.E. Tallman, S.C. Rasmussen, Synth. Met. 152 (2005) 137.

[93] S. Luzzati, A. Mozer, P. Denk, M.C. Scharber, M. Catellani, N.-O. Lupsac, F. Giacalone, J.L. Segura, N. Martin, H. Neugebauer, N.S. Sariciftci, Proc. SPIE 5215 (2004) 41.

[94] M. Catellani, S. Luzzati, N.-O. Lupsac, R. Mendichi, R. Consonni, A. Famulari, S.V. Meille, F. Giacalone, J.L. Segura, N. Martin, J. Mater. Chem. 14 (2004) 67.

[95] M. Catellani, S. Luzzati, N.-O. Lupsac, R. Mendichi, R. Consonni, F. Giacalone, J.L. Segura, N. Martín, Thin Solid Films 451–452 (2004) 2.

[96] M. Theander, A. Yartsev, D. Zigmantas, V. Sundström, W. Mammo, M.R. Andersson, O. Inganäs, Phys. Rev. B 61 (2000) 12957.

[97] J. Hou, C. Yang, Y. Li, Synth. Met. 153 (2006) 93.

[98] A. Gadisa, M. Svensson, M.R. Andersson, O. Inganäs, Appl. Phys. Lett. 84 (2004) 1609.

[99] E. Zhou, C. He, Z. Tan, C. Yang, Y. Li, J. Pol. Sci. A, Pol. Chem. 44 (2006) 4916.

[100] Y. Greenwald, G. Cohen, J. Poplawski, E. Ehrenfreund, S. Speiser, D. Davidor, J. Am. Chem. Soc. 118 (1996) 2980.

[101] T. Johansson, W. Mammo, M. Svensson, M.R. Andersson, O. Inganäs, J. Chem. Mater. 13 (2003) 1316.

[102] K.K. Stokes, K. Heuzé, R.D. McCullough, Macromolecules 36 (2003) 7114.

[103] S. Glenis, G. Horowitz, G. Tourillon, F. Garnier, Thin Solid Films 111 (1984) 93.

[104] Homepage of America Dye Sources, Inc.: ⟨http://www.adsdyes.com/⟩.

[105] F. Padinger, R.S. Rittberger, N.S. Sariciftci, Adv. Funct. Mater. 13 (2003) 85.

[106] G. Li, V. Shrotriya, J. Huang, Y. Yao, T. Moriarty, K. Emery, Y. Yang, Nat. Mater. 4 (2005) 864.

[107] P. Vanlaeke, G. Vanhoyland, T. Aernouts, D. Cheyns, C. Deibel, J. Manca, P. Heremans, J. Poortmans, Thin Solid Films 511–512 (2006) 358.

[108] V. Shotriya, G. Li, Y. Yao, C.-W. Chu, Y. Yang, Appl. Phys. Lett. 88 (2006) 073508 1-3.

[109] D. Chirvase, J. Parisi, J.C. Hummelen, V. Dyakonov, Nanotech 15 (2004) 1317.

[110] I. Riedel, V. Dyakonov, Phys. Stat. Solidi (a) 201 (2004) 1332.

[111] M. Drees, H. Hoppe, C. Winder, H. Neugebauer, N.S. Sariciftci, W. Schwinger, F. Schäffler, C. Topf, M.C. Scharber, Z. Zhu, R. Gaudiana, J. Mater. Chem. 15 (2005) 5158.

[112] K. Inoue, R. Ulbricht, P.C. Madakasira, W.M. Sampson, S. Lee, J. Gutierrez, J. Ferraris, A.A. Zakhidov, Proc. SPIE 5520 (2004) 256.

[113] Y. Kim, S.A. Choulis, J. Nelson, D.D.C. Bradley, S. Cook, J.R. Durrant, J. Mater. Sci. 40 (2005) 1371.

[114] B. Fan, P. Wang, L. Wang, G. Shi, Sol. Energy Mater. Sol. Cells 90 (2006) 3547.

[115] P. Schilinski, C. Waldauf, C.J. Brabec, Appl. Phys. Lett. 81 (2002) 3885.

[116] X. Yang, J. Loos, S.C. Veenstra, W.J.H. Verhees, M.M. Wienk, J.M. Kroon, M.A.J. Michels, R.A.J. Janssen, Nano Lett. 5 (2005) 579.

[117] J. Hou, Z. Fan, Y. Yan, Y. He, C. Yang, Y. Li, J. Am. Chem. Soc. 128 (2006) 4911.

[118] R. Cugola, U. Giovanella, P. Di Gianvincenzo, F. Bertini, M. Catellani, S. Luzzati, Thin Solid Films 511–512 (2006) 489.

[119] J.Y. Kim, S.H. Kim, H.-H. Lee, K. Lee, W. Ma, X. Gong, A.J. Heeger, Adv. Mater. 18 (2006) 572.

[120] A.G. Oumnov, V.Z. Mordkovich, Y. Takeuchi, Synth. Met. 121 (2001) 1581.

[121] S. Berson, R. De Bettignies, S. Guillerez, TNT2006, Grenoble, France, September 2006.

[122] S. Guillerez, R. de Bettignies, S. Berson, European conference on hybrid and organic solar cells, in: ECHOS'06, 28–30 June 2006, Paris, France, paper number 28-O1-3.

[123] D. Gebeyehu, C.J. Brabec, F. Padinger, T. Fromherz, J.J. Hummelen, D. Badt, H. Schindler, N.S. Sariciftci, Synth. Met. 118 (2001) 1.

[124] M. Trznadel, A. Pron, M. Zagorska, R. Chrzaszcz, J. Pielichowski, Macromolecules 31 (1998) 5051.

[125] S.E. Shaheen, C.J. Brabec, N.S. Sariciftci, F. Padinger, T. Fromherz, J.C. Hummelen, Appl. Phys. Lett. 78 (2001) 841.

[126] Z. Zhu, S. Hadjikyriacou, D. Waller, R. Gaudiana, J. Macromol. Sci. A: Pure Appl. Chem. 41 (2004) 1467.

[127] E. van Hauff, J. Parisi, V. Dyakonov, Thin Solid Films 511–512 (2006) 506.

[128] A. Swinnen, I. Haeldersmans, M. vande Ven, J. D'Haen, G. Vanhoyland, S. Aresu, M. D'Olieslaeger, J. Manca, Adv. Funct. Mater. 16 (2006) 760.

[129] Y. Kim, S. Cook, S.M. Tuladhar, S.A. Choulis, J. Nelson, J.R. Durrant, D.D.C. Bradley, M. Giles, I. McCulloch, C.-S. Ha, M. Ree, Nat. Mater. 5 (2006) 197.

[130] M. Theander, M.R. Andersson, O. Inganäs, Synth. Met. 101 (1999) 331.

[131] W.J.E. Beek, M.M. Wienk, R.A.J. Janssen, Adv. Funct. Mater. 16 (2006) 1112.

[132] G. Horowitz, F. Garnier, Sol. Energy Mater. 13 (1986) 47.

[133] J. Cao, J. Sun, G. Shi, H. Chen, Q. Zhang, D. Wang, M. Wang, Mater. Chem. Phys. 82 (2003) 44.

[134] A. Du Pasquier, H.E. Unalan, A. Kanwal, S. Miller, M. Chhowalla, Appl. Phys. Lett. 87 (2002) 203511 1-3.

[135] A. Cravino, G. Zerza, M. Maggini, S. Bucella, M. Svensson, M.R. Andersson, H. Neugebauer, C.J. Brabec, N.S. Sariciftci, Monatshefte Chem. 134 (2003) 519.

[136] A. Cravino, N.S. Sariciftci, J. Mater. Chem. 12 (2002) 1931.

[137] P.A. van Hal, R.A.J. Janssen, G. Lanzani, G. Cerullo, M. Zavelani-Rossi, S. De Silvestri, Chem. Phys. Lett. 345 (2001) 33.

[138] P. Wentzel, A. Du Pasquier, Mater. Res. Soc. Symp. Proc. 836 (2005) 75.

[139] N. Camaioni, G. Ridolfi, G. Casalbore-Miceli, G. Possamai, M. Maggini, Adv. Mater. 14 (2002) 1735.

[140] L. Chen, D. Godovsky, O. Inganäs, J.C. Hummelen, R.A.J. Janssen, M. Svensson, M.R. Andersson, Adv. Mater. 12 (2000) 1367.

[141] G. Dennler, H.-J. Prall, R. Koeppe, M. Egginger, R. Autengruber, N.S. Sariciftci, Appl. Phys. Lett. 89 (2006) 073502 1-3.

[142] L.B. Groenendaal, F. Louwet, P. Adriaensens, R. Carleer, D. Vanderzande, J. Gelan, Abst. Papers Am. Chem. Soc. PMSE 223 (2002) 59.

[143] F. Zhang, M. Johansson, M.R. Andersson, J.C. Hummelen, O. Inganäs, Adv. Mater. 14 (2002) 662.

[144] M. Granström, M. Berggren, O. Inganäs, Science 267 (1995) 1479.

[145] A.C. Arias, M. Granström, K. Petritsch, R.H. Friend, Synth. Met. 102 (1999) 953.

[146] C.S. Wang, M. Kilitziraki, L.O. Palsson, M.R. Bryce, A.P. Monkman, I.D.W. Samuel, Adv. Funct. Mater. 11 (2001) 47.

[147] I.F. Perepichka, E. Levillain, J. Roncali, J. Mater. Chem. 14 (2004) 1679.

[148] A. Berlin, G. Zotti, S. Zecchin, G. Schiavon, B. Vercelli, A. Zanelli, Chem. Mater. 16 (2004) 3667.

[149] J.-M. Raimundo, P. Blanchard, H. Brisset, S. Akoudad, J. Roncali, Chem. Commun. (2000) 939.

[150] G.A. Sotzing, C.A. Thomas, J.R. Reynolds, P.J. Steel, Macromolecules 31 (1998) 3750.

[151] F.L. Zhang, A. Gadissa, O. Inganäs, M. Svensson, M.R. Andersson, Appl. Phys. Lett. 84 (2004) 3906.

[152] B. Winther-Jensen, F.C. Krebs, Sol. Energy Mater. Sol. Cells 90 (2006) 123.

[153] L.A.A. Pettersson, S. Ghosh, O. Inganäs, Org. Elec. 3 (2002) 143.

[154] T. Aernouts, P. Vanlaerke, W. Geens, J. Poortmans, P. Heremans, S. Borghs, R. Mertens, R. Andriessen, L. Leenders, Thin Solid Films 451–452 (2004) 22.

[155] F. Wudl, M. Kobayashi, A.J. Heeger, J. Org. Chem. 49 (1984) 3382.

[156] M.P. Cava, M.V. Lakshmikantham, Acc. Chem. Res. 8 (1975) 139.

[157] M. Kobayashi, N. Colaneri, M. Boysel, F. Wudl, A.J. Heeger, J. Chem. Phys. 82 (1985) 5717.

[158] R. Kiebooms, I. Hoogmartens, P. Adriaensens, D. Vanderzande, J. Gelan, Macromolecules 28 (1995) 4961.

[159] P. Otto, J. Ladik, Synth. Metal 36 (1990) 327.

[160] H. Meng, F. Wudl, Macromolecules 34 (2001) 1810.

[161] R. van Asselt, I. Hoogmartens, D. Vanderzande, J. Gelan, P.E. Froehling, M. Aussems, O. Aagaard, R. Schellekens, Synth. Met. 74 (1995) 65.

[162] A.J. Hagan, S.C. Moratti, I.C. Sage, Synth. Met. 119 (2001) 147.

[163] I. Polec, A. Henckens, L. Goris, M. Nicolas, M.A. Loi, P.J. Adreaensens, L. Lutsen, J.V. Manca, D. Vanderzande, N.S. Sariciftci, J. Pol. Sci. A Pol. Chem 41 (2003) 1034.

[164] S.-A. Chen, C.-C. Lee, Polymer 37 (1996) 519.

[165] S.-A. Chen, C.-C. Lee, Pure & Appl. Chem. 67 (1995) 1983.

[166] L. Goris, M.A. Loi, A. Cravino, H. Neugebauer, N.S. Sariciftci, I. Polec, L. Lutsen, E. Andries, J. Manca, L. De Schepper, D. Vanderzande, Synth. Met. 138 (2003) 249.

[167] A. Henckens, M. Knipper, I. Polec, J. Manca, L. Lutsen, D. Vanderzande, Thin Solid Films 451–452 (2004) 572.

[168] S.E. Shaheen, D.L. Vangeneugden, R. Kiebooms, D. Vanderzande, T. Fromherz, F. Padinger, C.J. Brabec, N.S. Sariciftci, Synth. Met. 121 (2001) 1583.

[169] D.L. Vangeneugden, D.J.M. Vanderzande, J. Salbeck, P.A. van Hal, R.A.J. Janssen, J.C. Hummelen, C.J. Brabec, S.E. Shaheen, N.S. Sariciftci, J. Phys. Chem. 105 (2001) 11106.

[170] R. Kiebooms, F. Wudl, Synth. Met. 101 (1999) 40.

[171] R.H.L. Kiebooms, H. Goto, K. Akagi, Macromolecules 34 (2001) 7989.

[172] D.L. Vangeneugden, R.H.L. Kiebooms, D.J.M. Vanderzande, J.M.J.V. Gelan, Synth. Met. 101 (1999) 120.

[173] P. Bäuerle, G. Götz, U. Segelbacher, D. Huttenlocher, M. Mehring, Synth. Met. 55–57 (1993) 4768.

[174] G. Sonmez, H. Meng, F. Wudl, Chem. Mater. 15 (2003) 4923.

[175] H. Meng, D. Tucker, S. Chaffins, Y. Chen, R. Helgeson, B. Dunn, F. Wudl, Adv. Mater. 15 (2003) 146.

[176] A. Cravino, M.A. Loi, M.C. Scharber, C. Winder, H. Neugebauer, P. Denk, H. Meng, Y. Chen, F. Wudl, N.S. Sariciftci, Synth. Met. 137 (2003) 1435.

[177] D. Lorcy, M.P. Cava, Adv. Mater. 4 (1992) 562.

[178] D. Mühlbacher, H. Neugebauer, A. Cravino, N.S. Sariciftci, J.K.J. van Duren, A. Dhanabalan, P.A. van Hal, R.A.J. Janssen, J.C. Hummelen, Mol. Cryst. Liq. Cryst. 385 (2002) [205]/85–[212]/92.

[179] D. Mühlbacher, H. Neugebauer, A. Cravino, N.S. Sariciftci, Synth. Met. 137 (2003) 1361.

[180] A. Dhanabalan, J.L.J. van Dogen, J.K.J. van Duren, H.M. Janssen, P.A. van Hal, R.A.J. Janssen, Macromolecules 34 (2001) 2495.

[181] H.A.M. van Mullekom, J.A.J.M. Vekemans, E.W. Meijer, Chem. Eur. J. 4 (1998) 1235.

[182] H.A.M. van Mullekom, J.A.J.M. Vekemans, E.W. Meijer, Chem. Commun. (1996) 2163.

[183] C. Edder, P.B. Armstrong, K.B. Prado, J.M.J. Fréchet, Chem. Commun. (2006) 1965.

[184] A. Dhanabalan, P.A. van Hal, J.K.J. van Duren, J.L.J. van Dogen, R.A.J. Janssen, Synth. Met. 119 (2001) 169.

[185] C.J. Brabec, N.S. Sariciftci, J.C. Hummelen, Adv. Funct. Mater. 11 (2001) 15.

[186] C. Winder, G. Matt, J.C. Hummelen, R.A.J. Janssen, N.S. Sariciftci, C.J. Brabec, Thin Solid Films 403–404 (2002) 373.

[187] C.J. Brabec, C. Winder, N.S. Sariciftci, J.C. Hummelen, A. Dhanabalan, P.A. van Hal, R.A.J. Janssen, Adv. Funct. Mater. 12 (2002) 709.

[188] C. Winder, D. Mühlbacher, H. Neugebauer, N.S. Sariciftci, C. Brabec, R.A.J. Janssen, J.K. Hummelen, Mol. Cryst. Liq. Cryst. 385 (2002) [213]/93–[220]/100.

[189] M. Jayakannan, P.A. van Hal, R.A.J. Janssen, J. Pol. Sci. A Pol. Chem 40 (2002) 2360.

[190] E. Bundgaard, F.C. Krebs, Pol. Bull. 55 (2005) 157.

[191] M.M. Wienk, M.P. Struijk, R.A.J. Janssen, Chem. Phys. Lett. 422 (2006) 488.

[192] E. Bundgaard, S.E. Shaheen, F.C. Krebs, D. Ginley, Chem. Mater. (2007) (submitted).

[193] L.M. Campos, A. Tontcheva, S. Günes, G. Sonmez, H. Neugebauer, N.S. Sariciftci, F. Wudl, Chem. Mater. 17 (2005) 4031.

[194] M.M. Wienk, M.G.R. Turbiez, M.P. Struijk, M. Fonrodona, R.A.J. Janssen, Appl. Phys. Lett. 88 (2006) 153511 1-3.

[195] M. Pomerantz, B. Chaloner-Gill, L.O. Harding, J.J. Tseng, W.J. Pomerantz, J. Chem. Soc. Chem. Commun. (1992) 1672.

[196] D.D. Kenning, M.R. Funfar, S.C. Rasmussen, Polym. Preprints 42 (2001) 506.

[197] T. Yamamoto, A. Morita, Y. Miyazaki, T. Marayuma, H. Wakayama, Z. Zhou, Y. Nakamura, T. Kanbara, S. Sasaki, K. Kubota, Macromolecules 25 (1992) 1214.

[198] M. Shahid, R.S. Ashraf, E. Klemm, S. Sensfass, Macromolecules 39 (2006) 7844.

[199] M.T. Bernius, M. Inbasekaran, J. O'Brien, W. Wu, Adv. Mater. 12 (2000) 1737.

[200] G. Klaerner, R.D. Miller, Macroloecules 31 (1998) 2007.

[201] Q. Hou, Y. Xu, W. Yang, M. Yuan, J. Peng, Y. Cao, J. Mater. Chem. 12 (2002) 2887.

[202] G. Greczynski, M. Fahlman, W.R. Salaneck, N. Johansson, D.A. dos Santos, A. Dkhissi, J.L. Brédas, J. Chem. Phys. 116 (2002) 1700.

[203] M. Svensson, F. Zhang, S.C. Veenstra, W.J.H. Verhees, J.C. Hummelen, J.M. Kroon, O. Inganäs, M.R. Andersson, Adv. Mater. 15 (2003) 988.

[204] C. Shi, Y. Yao, Y. Yang, Q. Pei, J. Am. Chem. Soc. 128 (2006) 8980.

[205] R. Yang, R. Tian, J. Yan, Y. Zhang, J. Yang, Q. Hou, W. Yang, C. Zhang, Y. Cao, Macromolecules 38 (2005) 244.

[206] T. Yohannes, F. Zhang, M. Svensson, J.C. Hummelen, M.R. Andersson, O. Inganäs, Thin Solid Films 449 (2004) 152.

[207] Q. Zhou, Q. Hou, L. Zheng, X. Deng, G. Yu, Y. Cao, Appl. Phys. Lett. 84 (2004) 1653.

[208] O. Inganäs, M. Svensson, F. Zhang, A. Gadisa, N.K. Persson, X. Wang, M.R. Andersson, Appl. Phys. A 79 (2004) 31.

[209] L.M. Andersson, O. Inganäs, Appl. Phys. Lett. 88 (2006) 082103 1-3.

[210] F. Zhang, K.G. Jespersen, C. Björström, M. Svensson, M.R. Andersson, V. Sundström, K. Magnusson, E. Moons, A. Yartsev, O. Inganäs, Adv. Funct. Mater. 16 (2006) 667.

[211] R. Pacios, D.D.C. Bradley, J. Nelson, C.J. Brabec, Synth. Met. 137 (2003) 1469.

[212] J.-I. Lee, G. Klaerner, M.H. Davey, R.D. Miller, Synth. Met. 102 (1999) 1087.

[213] X. Wang, E. Perzon, F. Oswald, F. Langa, S. Admassie, M.R. Andersson, O. Inganäs, Adv. Funct. Mater. 15 (2005) 1665.

[214] X. Wang, E. Perzon, J.L. Delgado, P. de la Cruz, F. Zhang, F. Langa, M. Andersson, O. Inganäs, Appl. Phys. Lett. 85 (2004) 5081.

[215] F. Zhang, E. Perzon, X. Wang, W. Mammo, M.R. Andersson, O. Inganäs, Adv. Funct. Mater. 15 (2005) 745.

[216] E. Perzon, X. Wang, F. Zhang, W. Mammo, J.L. Delgado, P. de la Cruz, O. Inganäs, F. Langa, M.R. Andersson, Synth. Met. 154 (2005) 53.

[217] X. Wang, E. Perzon, W. Mammo, F. Oswald, S. Admassie, N.-K. Persson, F. Langa, M.R. Andersson, O. Inganäs, Thin Solid Films 511–512 (2006) 576.

[218] M. Chen, E. Perzon, N. Robisson, S.K.M. Jönsson, M.R. Andersson, M. Fahlman, M. Berggren, Synth. Met. 146 (2004) 233.

[219] K.G. Jespersen, F. Zhang, A. Gadisa, V. Sundström, A. Yartsev, O. Inganäs, Org. Elec. 7 (2006) 235.

[220] E. Perzon, X. Wang, S. Admassie, O. Inganäs, M.R. Andersson, Polymer 47 (2006) 4261.

[221] M. Chen, X. Crispin, E. Perzon, M.R. Andersson, T. Pullerits, M. Berggren, Appl. Phys. Lett. 87 (2005) 252105 1-3.

[222] A. Gadisa, X. Wang, S. Admassie, E. Perzon, F. Oswald, F. Langa, M.R. Andersson, O. Inganäs, Org. Elec. 7 (2006) 195.

[223] M.M. Wienk, J.M. Kroon, W.J.H. Verhees, J. Knol, J.C. Hummelen, P.A. van Hal, R.A.J. Janssen, Angew. Chem. Int. Ed. 42 (2003) 3371.

[224] D.M. Johansson, T. Granlund, M. Theander, O. Inganäs, M.R. Andersson, Synth. Met. 121 (2001) 1761.

[225] S.K. Lee, N.S. Cho, J.H. Kwak, K.S. Lim, H.-K. Shim, D.-H. Hwang, C.J. Brabec, Thin Solid Films 511–512 (2006) 157.

[226] I.T. Kim, S.W. Lee, M.H. Kwak, S.J. Kim, G.B. Park, H.W. Kim, Polym. Preprints 45 (2004) 218.

[227] I.T. Kim, S.W. Lee, H.S. Park, T.H. Kwak, C.M. Lee, S.Y. Kim, Polym. Preprints 44 (2003) 931.

[228] I.T. Kim, S.W. Lee, J.Y. Lee, Polym. Preprints 44 (2003) 1163.

[229] C. Taliani, G. Ruani, R. Zamboni, A. Bolognesi, M. Catellani, S. Destri, W. Porzio, P. Ostoja, Synth. Met. 28 (1989) C507.

[230] C. Taliani, R. Zamboni, G. Ruani, in: J. Messier, F. Kajzar, P. Prasad, D. Ulrich (Eds.), Nonlinear Optical Effects in Organic Polymers, vol. 162, Kluwer Academic Publishers, Dordrecht, 1988, pp. 159–172.

[231] C. Arbizzani, M. Catellani, M. Mastragostino, M.G. Cerroni, J. Electroanl. Chem. 423 (1997) 23.

[232] A. Cravino, H. Neugebauer, S. Luzzati, M. Catellani, N.S. Sariciftci, J. Phys. Lett. B 105 (2001) 46.

[233] S. Tanaka, Y. Yamashita, Synth. Met. 55–57 (1993) 1251.

[234] S. Tanaka, Y. Yamashita, Synth. Met. 69 (1995) 599.

[235] M. Pomerantz, X. Gu, S.X. Zhang, Macromolecules 34 (2001) 1817.

[236] M. Pomerantz, X. Gu, Synth. Met. 84 (1997) 243.

[237] B. Lee, V. Seshadri, G.A. Sotzing, Polym. Preprints 46 (2005) 1010.

[238] K. Lee, G.A. Sotzing, Macromolecules 34 (2001) 5746.

[239] G.A. Sotzing, K. Lee, Polym. Preprints 85 (2001) 604.

[240] B. Lee, M.S. Yavuz, G.A. Sotzing, Polym. Preprints 46 (2005) 860.

[241] A. Kumar, G.A. Sotzing, Polym. Preprints 46 (2005) 969.

[242] A. Kumar, Z. Buyukmumcu, G.A. Sotzing, Macromolecules 39 (2006) 2723.

[243] B. Lee, V. Seshadri, G.A. Sotzing, Synth. Met. 152 (2005) 177.

[244] B. Lee, V. Seshadri, G.A. Sotzing, Langmuir 21 (2005) 10797.

[245] M. Hanack, U. Schmid, U. Röhrig, J.-M. Toussaint, C. Adant, J.-L. Brédas, Chem. Ber. 126 (1993) 1487.

[246] N.-O. Lupsac, M. Catellani, S. Luzzati, Mol. Cryst. Liq. Cryst. 385 (2002) [241]/121–[248]/128.

[247] C.-G. Wu, C.-W. Hsieh, D.-C. Chen, S.-J. Chang, K.-Y. Chen, Synth. Met. 155 (2005) 618.

[248] S. Das, A. Ajayaghosh, K.R. Gopidas, D. Ramaiah, K.G. Thomas, Metals Mater. Proces. 13 (2001) 351.

[249] J. Eldo, A. Ajayaghosh, Chem. Mater. 14 (2002) 410.

[250] G. Brocks, A. Tol, J. Phys. Chem. 100 (1996) 1838.

[251] E.E. Havinga, W. ten Hoeve, H. Wynberg, Synth. Met. 55–57 (1993) 299.

[252] H. Cheng, R.L. Elsenbaumer, J. Chem. Soc. Chem. Commun. (1995) 1451.

[253] I.T. Kim, R.L. Elsenbaumer, Macromolecules 33 (2000) 6407.

[254] W.J. Mitchell, C. Pena, P.L. Burn, J. Mater. Chem. 12 (2001) 200.

[255] A. Henckens, K. Colladet, S. Fourier, T.J. Cleij, L. Lutsen, J. Gelan, D. Vanderzande, Macromolecules 38 (2005) 19.

[256] L.H. Nguyen, S. Günes, H. Neugebauer, N.S. Sariciftci, F. Banishoeib, A. Henckens, T. Cleij, L. Lutsen, D. Vanderzande, Sol. Energy Mater. Sol. Cells 90 (2006) 2815.

[257] K. van de Wetering, C. Brochon, C. Ngov, G. Hadziioannou, Macromolecules 39 (2006) 4289.

[258] I.T. Kim, R.L. Elsenbaumer, Chem. Commun. (1998) 327.

[259] Q. Zhang, Y. Li, M. Yang, J. Mater. Sci. 39 (2004) 6089.

[260] Q. Zhang, Y. Li, M. Yang, Synth. Met. 146 (2004) 69.

[261] Q. Zhang, M. Yang, P. Wu, H. Ye, X. Lui, Synth. Met. 156 (2006) 135.

[262] Q. Zhang, J. Feng. K. Lui, D. Zhu, M. Yang, H. Ye, X. Lui, Synth. Met. 156 (2006) 804.

[263] K. Colladet, M. Nicolas, L. Goris, L. Lutsen, D. Vanderzande, Thin Solid Films 451–452 (2004) 7.

[264] T. Yamamoto, M. Arai, H. Kokubo, S. Sasaki, Macromolecules 36 (2003) 7986.

[265] R. Demadrille, M. Firon, J. Leroy, P. Rannou, A. Pron, Adv. Funct. Mater. 15 (2005) 1547.

[266] M.B. Zaman, D.F. Perepichka, Chem. Commun. (2005) 4187.

[267] B.D. Reeves, C.R.G. Grenier, A.A. Argun, A. Cirpan, T.D. McCarley, J.R. Reynolds, Macromolecules 37 (2004) 7559.

[268] L.M. Campos, A.J. Mozer, S. Günes, C. Winder, H. Neugebauer, N.S. Sariciftci, B.C. Thompson, B.D. Reeves, C.R.G. Grenier, J.R. Reynolds, Sol. Energy Mater. Sol. Cells 90 (2006) 3531.

[269] D. Mühlbacher, M. Scharber, M. Morana, Z. Zhu, D. Waller, R. Gaudiana, C.J. Brabec, Adv. Mater. 18 (2006) 2284.

[270] D. Mühlbacher, M. Scharber, M. Morana, Z. Zhu, D. Waller, R. Gaudiana, C.J. Brabec, Adv. Mater. 18 (2006) 2284, correction.

[271] G. Sonmez, C.K.F. Shen, Y. Rubin, F. Wudl, Adv. Mater. 17 (2005) 897.

[272] J. Cremer, P. Bäuerle, J. Mater. Chem. 16 (2006) 874.

[273] F.C. Krebs, R.B. Nyberg, M. Jørgensen, Chem. Mater. 16 (2004) 1313.

[274] K.T. Nielsen, K. Bechgaard, F.C. Krebs, Macromolecules 38 (2005) 658.

[275] K.T. Nielsen, K. Bechgaard, F.C. Krebs, Synthesis 10 (2006) 1639.

[276] V. Duprez, M. Biancardo, H. Spanggaard, F.C. Krebs, Macromolecules 38 (2005) 10436.

[277] J. Alstrup, K. Norrman, M. Jørgensen, F.C. Krebs, Sol. Energy Mater. Sol. Cells 90 (2006) 2777.

[278] K. Norrman, J. Alstrup, M. Jørgensen, F.C. Krebs, Surf. Interface Anal. 38 (2006) 1302.

[279] K. Norrman, N.B. Larsen, F.C. Krebs, Sol. Energy Mater. Sol. Cells 90 (2006) 2793.

[280] K. Norrman, F.C. Krebs, Sol. Energy Mater. Sol. Cells 90 (2006) 213.

[281] M. Lira-Cantu, F.C. Krebs, Sol. Energy Mater. Sol. Cells 90 (2006) 2076.

[282] M. Lira-Cantu, K. Norrman, J.W. Andreasen, F.C. Krebs, Chem. Mater. 18 (2006) 5684.